Available online at www.sciencedirect.com
ScienceDirect
Polymer 48 (2007) 6097–6114
polymer
www.elsevier.com/locate/polymer

Pure and mixed gas CH_4 and n-C_4H_{10} sorption and dilation in poly(1-trimethylsilyl-1-propyne)

Roy D. Raharjo [a], Benny D. Freeman [a,*], Edgar S. Sanders [b]

[a] *University of Texas at Austin, Department of Chemical Engineering, Center for Energy and Environmental Resources, 10100 Burnet Road, Building 133, Austin, TX 78758, USA*

[b] *Air Liquide Research and Development, 200 GBC Drive, Newport, DE 19702, USA*

Received 23 June 2007; accepted 25 July 2007
Available online 1 August 2007

Abstract

Pure and mixed gas n-C_4H_{10} and CH_4 sorption and dilation in poly(1-trimethylsilyl-1-propyne) (PTMSP) are reported at temperatures ranging from −20 to 35 °C. The presence of n-C_4H_{10} in the mixture considerably reduces CH_4 solubility. For example, CH_4 solubility (in the limit of zero CH_4 fugacity) at 25°C decreases from 4.0 (pure gas) to 0.78 cm^3(STP)/(cm^3 polymer atm) in the presence of n-C_4H_{10} at an activity of 0.60. At −20 °C, CH_4 solubility decreases by almost an order of magnitude, from 10.2 (pure gas) to 1.22 cm^3(STP)/(cm^3 polymer atm) in the presence of n-C_4H_{10} at an activity of 0.61. In contrast, n-C_4H_{10} mixture sorption properties are not measurably affected by the presence of CH_4. The dual mode sorption model parameters for CH_4 and n-C_4H_{10} in PTMSP were determined from pure and mixed gas sorption measurements, and this model can adequately describe the sorption data. The n-C_4H_{10}/CH_4 mixed gas solubility selectivity in PTMSP decreases as temperature increases and as n-C_4H_{10} activity increases. For example, at 25 °C, the n-C_4H_{10}/CH_4 solubility selectivity decreases from 250 to 120 as n-C_4H_{10} activity increases from 0.02 to 0.25. At −20 °C and an n-C_4H_{10} activity of 0.24, the n-C_4H_{10}/CH_4 solubility selectivity is 590. Penetrant-induced volume dilation of PTMSP can be adequately modeled by assuming that all swelling is caused by penetrant molecules sorbed in the polymer's dense equilibrium region (*i.e.*, the Henry's law region) during sorption. However, the best fit partial molar volumes in the Henry's law region for the dilation data are considerably lower than the penetrant partial molar volumes in liquids, suggesting that further theoretical efforts are needed to develop predictive models of volume dilation in high free volume glassy polymers.

Keywords: Mixed gas solubility; Dilation; Poly(1-trimethylsilyl-1-propyne) (PTMSP)

1. Introduction

Higher hydrocarbon (C_{3+}) removal from natural gas is required to reduce the dewpoint and heating value to pipeline specifications, prevent condensation during transportation, and recover valuable higher hydrocarbons for use as chemical feedstocks [1,2]. Membrane separation has recently emerged as a potential alternative to current technologies (*e.g.*, condensation), which are capital- and energy-intensive, for this separation [1]. For economic reasons, membranes for this application should be vapor selective materials so that the methane product is retained at high pressure [1]. Such polymers filter penetrant molecules based primarily on relative solubility and are more permeable to larger, more condensable organic vapors (*e.g.*, n-C_4H_{10}) than to smaller, less condensable, permanent gases (*e.g.*, CH_4).

While there are many reports of pure gas sorption and transport properties in vapor selective materials [3–9], gas mixture separation properties, which are required for estimating membrane separation performance, are less often reported [10–12]. Differences between pure and mixed gas permeability coefficients in vapor selective polymers have been reported [10,11]. For example, Pinnau et al. observed a significant decrease in hydrogen permeability in poly(1-trimethylsilyl-1-propyne)

* Corresponding author. Tel.: +1 512 232 2803; fax: +1 512 232 2807.
E-mail address: freeman@che.utexas.edu (B.D. Freeman).

0032-3861/$ - see front matter © 2007 Elsevier Ltd. All rights reserved.
doi:10.1016/j.polymer.2007.07.057

(PTMSP) when the mixtures contained propane, which increased the selectivity of propane over hydrogen [11]. Pure hydrogen permeability was 21,000 Barrer, but it decreased to 1100 Barrer in a mixture containing propane at a relative propane pressure (p/p_{sat}) of 0.83 [11]. The propane permeability increased slightly, from 25,000 to 29,000 Barrer, as the relative propane pressure increased from 0 to 0.83 [11]. As a result, the propane/hydrogen selectivity increased from about 1.4, based on pure gas measurements, to approximately 26 in a mixture at high relative propane pressure [11]. In a similar study, Pinnau and Toy reported an increase in *n*-butane/methane selectivity in PTMSP, from 5 in pure gas to 30 in a mixture of 2 mol% *n*-butane in methane at 250 psig feed pressure and 23 °C [13]. In mixture permeation measurements, methane permeability was only 1800 Barrer, almost 10 times less than the pure gas value (15,400 Barrer) [13]. The larger, more soluble, *n*-C_4H_{10}, the authors speculated, partially blocked the CH_4 permeation pathway, decreasing its diffusion coefficient [11,13]. Neither study, however, provided mixture solubility or mixture diffusion data. Without such data, it is impossible to evaluate these assumptions, and, to the best of our knowledge, the literature contains no such data for PTMSP.

This study presents pure and mixed gas CH_4/*n*-C_4H_{10} solubility and dilation properties of PTMSP. This particular mixture was selected due to interest in using membranes for higher hydrocarbon removal from natural gas [1]. CH_4 is the primary product in natural gas, and *n*-C_4H_{10} serves as a model marker molecule for higher hydrocarbons. Temperatures explored in this study range from −20 to 35 °C. The lower limit, −20 °C, is representative of the dewpoint requirement of pipeline-grade natural gas [1]. Some condensation processes used to remove higher hydrocarbons operate in this temperature range [2]. The upper limit, 35 °C, is in the range of common operating temperatures for membrane gas separation processes [1]. A separate study will report CH_4/*n*-C_4H_{10} mixture permeability in PTMSP to complement these results. Together, the mixture permeability and sorption data permit calculation of mixture diffusion coefficients to determine whether observed differences in mixture and pure gas permeability values are due to differences in pure and mixed gas solubility, diffusivity, or both.

2. Background

Gas solubility in a polymer is defined as [14]:

$$S = \frac{C}{f} \tag{1}$$

where C is the equilibrium concentration of gas sorbed in the polymer when the fugacity of the gas phase in contact with the polymer is f. Often, when the gas is ideal, fugacity is replaced by pressure (or partial pressure, in the case of mixtures) in Eq. (1). In this study, fugacity is used to account for gas phase nonidealities because these effects are significant, particularly for *n*-C_4H_{10}, in the mixtures considered [12].

The temperature dependence of solubility is usually described as follows [15]:

$$S = S_o \exp\left(\frac{-\Delta H_S}{RT}\right) \tag{2}$$

where S_o is a pre-exponential factor, ΔH_S is the enthalpy of sorption, R is the universal gas constant, and T is the absolute temperature. Since sorption in polymer is typically viewed as a two step process involving penetrant condensation from a gas-like density to a liquid-like density followed by mixing condensed penetrant molecules with polymer segments, the enthalpy of sorption can be viewed as a sum of the enthalpy changes for these two steps [16]:

$$\Delta H_S = \Delta H_{cond} + \Delta H_{mix} \tag{3}$$

where ΔH_{cond} and ΔH_{mix} are the enthalpy changes associated with penetrant condensation and mixing, respectively [16].

Sorption in a glassy polymer is often described using the dual mode sorption model, where penetrant molecules are viewed as being partitioned between the dense equilibrium structure of the polymer (Henry's law region) and the non-equilibrium excess volume (Langmuir region). The model for pure gas sorption is given by [17]:

$$C = C_D + C_H = k_D f + \frac{C'_H b f}{1 + b f} \tag{4}$$

where C_D and C_H are the concentrations of penetrant sorbed in the Henry's law and Langmuir regions, respectively; k_D is the Henry's law constant, C'_H is the Langmuir sorption capacity, and b is the Langmuir affinity constant.

Competitive effects have been observed during gas mixture sorption in glassy polymers [18,19]. Penetrant molecules compete for the limited number of sorption sites available in the non-equilibrium excess volume (*i.e.*, Langmuir sites), which leads to lower gas solubilities in mixtures than in pure gas studies [19]. Within the context of the dual mode model, the fraction of unrelaxed free volume that each penetrant can occupy depends on the penetrant affinity constant (b) and the fugacities of individual components [19]. Sanders, in his Ph.D. dissertation, extended the dual mode model to binary mixtures [18]. Based on this model, sorption of a binary mixture of gases A and B in a polymer will result in concentrations of A and B in the glassy polymer, C_A and C_B, respectively, given by the following equations [18]:

$$C_A = k_{D_A} f_A + \frac{C'_{H_A} b_A f_A}{1 + b_A f_A + b_B f_B} \tag{5}$$

$$C_B = k_{D_B} f_B + \frac{C'_{H_B} b_B f_B}{1 + b_B f_B + b_A f_A} \tag{6}$$

where f_A and f_B are the fugacities of A and B, respectively, in the gas phase in contact with the polymer.

3. Experimental

3.1. Materials

Poly(1-trimethylsilyl-1-propyne) (PTMSP) was kindly supplied by Air Products, Inc. (St. Louis, MO). Dense films of PTMSP were prepared by casting a polymer solution in a flat-bottomed glass dish at ambient conditions. The polymer solution contained 2 wt% PTMSP in toluene. After drying, which generally required about 24 h at ambient conditions, the samples were stored in liquid methanol at ambient conditions to inhibit physical aging [20]. The films were removed from methanol and dried at ambient conditions for 24 h before being used in experiments. Film thicknesses were determined with a digital micrometer (Mitutoyo) readable to ± 1 μm. Samples for the sorption and dilation measurements were approximately 100 μm thick. The density of the PTMSP films at 25 °C was approximately 0.73 ± 0.01 g/cm^3, determined by measuring the difference in the weight of a film in water and in air.

Chemical-grade CH_4 and n-C_4H_{10} (99% purity) were purchased from Air Gas Southwest Inc. (Corpus Christi, TX). Certified 2, 4, 6, and 8 mol% n-C_4H_{10}/CH_4 gas mixtures were purchased from Air Liquide America Corporation (Houston, TX). All gases were used as received.

3.2. Sorption measurements

Pure and mixed gas solubility coefficients were determined using an apparatus based on the barometric, pressure-decay method described previously [12]. The system consists of three interconnected cells: the charge volume, the polymer-containing volume, and the sampling volume. Each cell is equipped with a Super TJE pressure transducer from Honeywell Sensotec (Columbus, OH), which has an accuracy of 0.05% of full scale. The GC is a type 6890 from Agilent Technology (Santa Clara, CA) equipped with two columns: (1) 15 m × 530 μm, 5% phenyl/methyl siloxane, 3.0 μm film thickness, and (2) 30 m × 530 μm, CarboPLOT, 1.5 μm film thickness. A flame ionization detector (FID) connected to the first column is used to determine the composition of CH_4 and n-C_4H_{10} in the mixtures.

For pure gas sorption measurements, only two volumes, the charge volume and the polymer-containing volume, were utilized [12]. The PTMSP sample was degassed by maintaining the sorption system under vacuum overnight before each measurement. Initially, a desired amount of penetrant gas was added to the charge volume. After a steady pressure reading was obtained, the penetrant gas was expanded into the chamber containing the polymer sample and allowed to equilibrate. Once the pressure was constant, additional penetrant was admitted into the charge volume and then expanded to the polymer-containing volume, and equilibrium was reestablished. In this incremental manner, the amount of gas sorbed in the polymer as a function of penetrant fugacity/pressure was determined using mass balance calculations.

The mixed gas experiments involve adding only pure gases to the polymer-containing volume. This method allows the partial pressure of one component to be held relatively constant during the experiment. Pure n-C_4H_{10} was first added to the charge volume and then expanded into the polymer-containing volume. This step was repeated until a desired pressure in the polymer-containing volume was achieved. After evacuating n-C_4H_{10} from the charge volume, pure CH_4 was admitted into the charge volume and then expanded into the polymer-containing volume. A sufficient pressure difference was maintained between the polymer-containing volume and the charge volume to avoid n-C_4H_{10} backflow into the charge volume when the gas in the charge volume was admitted to the polymer-containing volume. After establishing equilibrium in the polymer-containing volume between the polymer and the gas mixture, a small amount of the gas mixture from the polymer-containing volume was expanded into the sampling volume and injected into the GC. Once the pressure in the polymer-containing volume was stable, additional CH_4 was added. Equilibrium was reestablished, and a small amount (less than 1% of the material in the gas phase, accounted for in the material balance) of the gas mixture in the polymer-containing volume was again injected into the GC through the sampling volume. Equilibrium between CH_4, n-C_4H_{10}, and the polymer in the polymer-containing volume was achieved after 24 h at most. The detailed procedure for mixed gas sorption measurements has been described previously [12].

No hysteresis effects were observed during the sorption measurements. Pure gas CH_4 sorption isotherms determined before and after pure gas sorption studies of n-C_4H_{10} were essentially the same, consistent with previous findings for PTMSP by Merkel et al. [5]. Because physical aging can decrease the penetrant solubility values in the polymer over time [20], pure gas sorption isotherms of CH_4 and n-C_4H_{10} were determined before every mixture sorption measurement. If significant physical aging effects were found, the polymer samples were rejuvenated by immersing them in liquid methanol for 24 h, then drying at ambient 24 h before measurements were taken.

3.3. Dilation measurements

Pure and mixed gas dilation measurements were performed using an apparatus based on a design by Fleming and Koros [21]. The device monitors one coordinate dimension of a polymer film during sorption. A strip of polymer was placed in the Jerguson gauge, where it was unconstrained in its ability to elongate: it was guided by a wire track that allowed the polymer to dilate freely along its length but precluded curling. The length of the polymer strip (*i.e.*, *x*-direction) was monitored by a COHU (model 4915-2000) CCD camera (San Diego, CA), which recorded digital images of the sample as a function of time. The minimum change in length detectable with this device is 0.017 mm; the sample used for the length (*i.e.*, *x*-direction) dilation measurements was approximately 90 mm long. More detailed information regarding the digital image capture and analysis protocols was reported by McDowell

et al. [22]. A water jacketed glass vessel connected to a temperature controller (Thermo Neslab) was used to control temperature. Most of the measurements utilized a pressure gauge (model CM) from Heise (Stratford, CT) with a full scale reading of 700 psia and an accuracy of 0.1% of full scale. For pure gas n-C_4H_{10} dilation measurements, a digital pressure gauge (model PM, also from Heise) with higher accuracy (0.025% of full scale, where the full scale reading was 300 psig) was used. The overall dimensions of dilation samples were 90 mm × 5 mm × 120 μm, in the x-, y-, and z-direction, respectively.

To check for isotropic expansion, thickness (*i.e.*, z-direction) dilation measurements were performed using a similar setup. However, for these measurements, the polymer sample in the Jerguson gauge was repositioned so that the camera monitored the cross-section of the film [23]. A smaller but thicker PTMPS film (100 mm × 100 mm × 200 μm) was used to reduce the chance of sample curling, and a longer focal length lens was used to improve accuracy. The minimum detectable thickness change using this setup was 0.008 mm.

For polymer dilation measurements in gas mixtures, which were used to complement the mixed gas sorption isotherms [12], a certified gas mixture was fed directly into the dilatometer. Due to the high dilation chamber to polymer sample volume ratio (~700), the amount of gas sorbed by the polymer were very small compared to that in the chamber, so any changes in gas mixture composition during the experiment was negligible [12]. At low temperatures, a constant flow of dry nitrogen was maintained in the enclosed area surrounding the system to prevent moisture from condensing on the glass surface of the dilatometer through which experimental measurements were made.

Unlike the sorption measurements, a small hysteresis effect was observed during the dilation measurements. The polymer sample tends to dilate more following dilation studies involving pure n-C_4H_{10} or mixtures containing n-C_4H_{10}. To eliminate hysteresis effects, between dilation measurements, polymer films were immersed in liquid methanol for 24 h and then dried at ambient conditions for 24 h before the next dilation measurement.

Two large sheets of PTMSP films (6.59 cm × 6.61 cm × 300 μm and 4.74 cm × 4.72 cm × 300 μm) were dilated in liquid methanol solution for 24 h to investigate the magnitude of the polymer width (*i.e.*, y-direction) dilation relative to that of the length (*i.e.*, x-direction) dilation. The initial (dry) and dilated (in pure liquid methanol) length and width of the films were determined using a Vernier caliper with ±0.01 cm accuracy.

4. Results and discussion

4.1. Pure gas solubility

Fig. 1 presents pure gas CH_4 sorption isotherms in PTMSP as a function of fugacity and temperature. The sorption isotherms are slightly concave to the pressure axis, which is common for sorption in glassy polymers [5]. The dashed line is the pure gas CH_4 sorption isotherm in PTMSP at 35 °C previously reported by Merkel et al. [5]. It is in good agreement with the pure gas CH_4 sorption isotherm at 35 °C in this study.

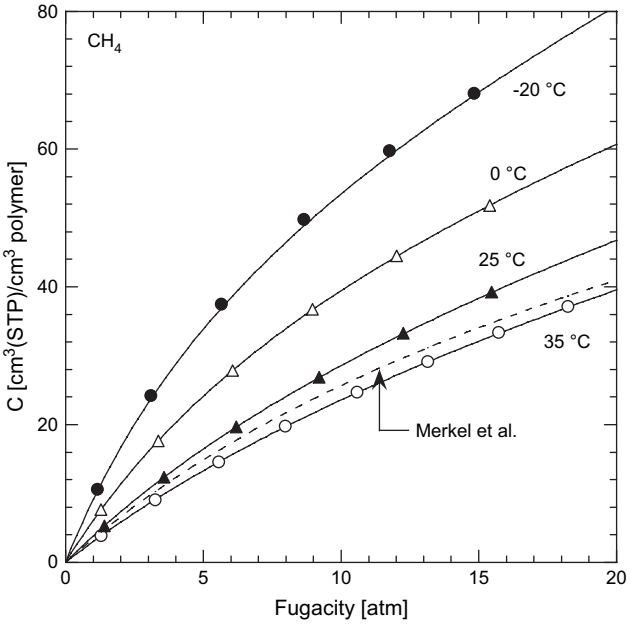

Fig. 1. CH_4 pure gas sorption isotherm as a function of CH_4 fugacity and temperature. The dashed line represents the CH_4 pure gas isotherm in PTMSP at 35 °C reported by Merkel et al. [5]. The solid lines are from the dual mode sorption model using parameters from Table 1.

Fig. 2(a) presents pure gas n-C_4H_{10} sorption isotherms in PTMSP as a function of fugacity and temperature. The sorption isotherms are concave to the pressure axis at low pressure. At high pressure, the isotherms are linear, indicating saturation of the Langmuir sites. The isotherm at 35 °C is in good agreement with that previously reported by Morisato et al. [6]. Fig. 2(b) presents the pure gas n-C_4H_{10} sorption isotherms as a function of activity, which is defined as the ratio of fugacity to the saturation fugacity at a given temperature (f/f_{sat}) [12]. The saturation fugacity is the fugacity at the saturation pressure (p_{sat}), and p_{sat} is estimated using the Wagner equation [12,24]. When plotted as a function of activity, the isotherms at high activity exhibit similar slopes (*i.e.*, activity-normalized k_D values are essentially independent of temperatures).

The pure gas sorption isotherms can be described by the dual mode model. Table 1 presents the dual mode parameters obtained by a nonlinear least squares fit of Eq. (4) to the experimental data. The uncertainties were estimated according to the propagation of errors method [25]. Although the b value for CH_4 at 35 °C in this study (0.051 ± 0.005 atm^{-1}) agrees with that reported by Merkel et al. (0.05 atm^{-1}) [5], our k_D value (0.86 ± 0.05 cm^3(STP)/(cm^3 atm)) is higher than theirs (0.50 cm^3(STP)/(cm^3 atm)), and our C'_H value (44 ± 5 cm^3(STP)/cm^3) is lower than Merkel et al.'s value (62 cm^3(STP)/cm^3) [5]. These discrepancies are probably due to the difficulty of obtaining a unique set of dual mode parameters for light gas sorption in glassy polymers when a limited pressure range is explored [5]. The maximum pressure in the present study is 18 atm. Merkel et al. measured the CH_4 isotherm at

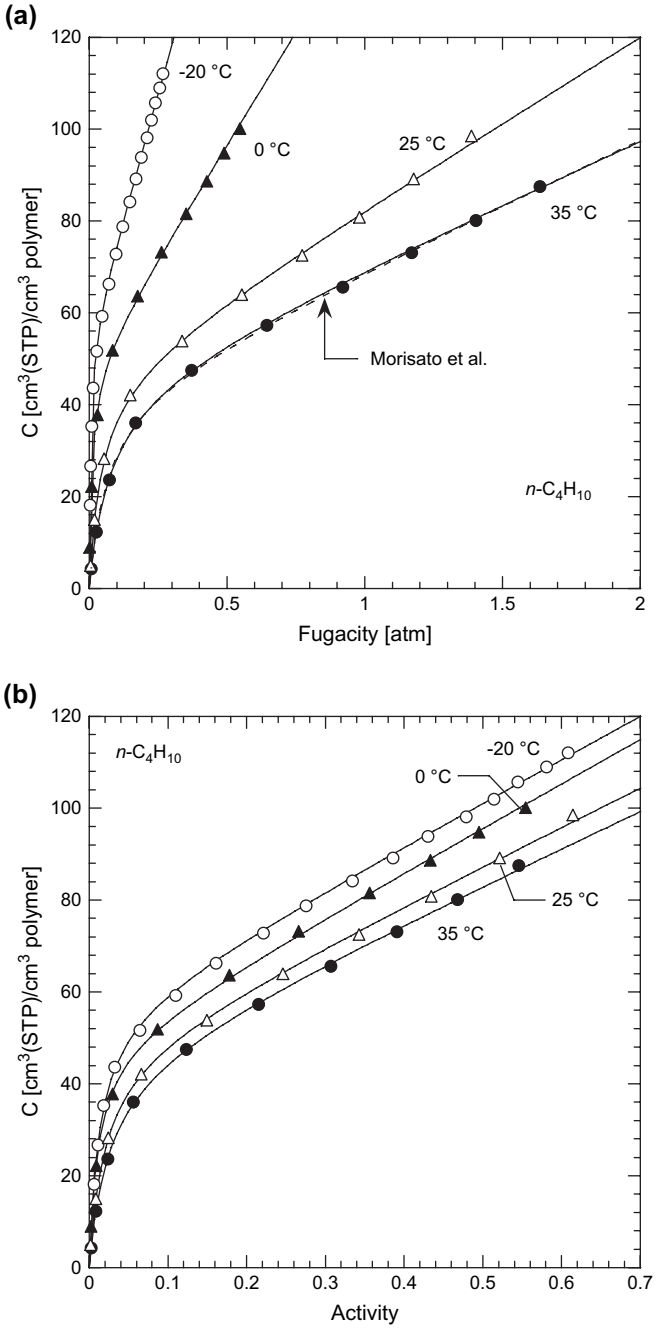

Fig. 2. n-C_4H_{10} pure gas sorption isotherm as a function of (a) n-C_4H_{10} fugacity and (b) n-C_4H_{10} activity (f/f_{sat}). The dashed line represents the n-C_4H_{10} pure gas sorption isotherm in PTMSP at 35 °C reported by Morisato et al. [6]. The solid lines are from the dual mode sorption equation using parameters from Table 1. For n-C_4H_{10}, f_{sat} values are 3.00, 2.26, 0.99, and 0.44 atm at 35, 25, 0, and −20 °C, respectively [24].

pressures up to 25 atm [5]. In these pressure ranges, the Langmuir sites in PTMSP are not saturated (*i.e.*, bf is not much greater than unity). Due to the lack of curvature in the CH_4 sorption isotherms, the estimated dual mode parameters are less reliable than those for n-C_4H_{10}, where the more strongly curved isotherms permit a more reliable estimate of a unique set of dual mode parameters. The n-C_4H_{10} parameters in this study are similar to those previously reported by Morisato et al. [6] Their k_D, C'_H, and b values of n-C_4H_{10} in PTMSP at 35 °C are 28 cm^3(STP)/(cm^3 atm), 43 cm^3(STP)/cm^3, and 15 atm^{-1}, respectively [6]; our values at the same temperature are 27 ± 2 cm^3(STP)/(cm^3 atm), 45 ± 2 cm^3(STP)/cm^3, and 13 ± 1 atm^{-1}. In general, k_D, C'_H, and b values increase as temperature decreases. k_D increases mainly because the penetrant condensability increases with decreasing temperature. For example, k_D of n-C_4H_{10} increases from 27 to 211 cm^3(STP)/(cm^3 atm) as temperature decreases from 35 to −20 °C. However, when corrected for the influence of penetrant condensability, the k_D values are essentially independent of temperature, which is also apparent from the slopes of the isotherms at higher activity in Fig. 2(b). Activity-based k_D values (*i.e.*, $k_D f_{sat}$) for n-C_4H_{10} at 35, 25, 0, and −20 °C are 80 ± 7, 84 ± 7, 96 ± 8, 93 ± 8 cm^3(STP)/cm^3, respectively. C'_H increases as temperature decreases, which is consistent with the fact that non-equilibrium excess volume in a glass polymer should increase as temperature decreases or as the difference between the temperature of the experiment and the glass transition temperature ($T - T_g$) increases [5]. In general, activity-based b values (*i.e.*, bf_{sat}) of n-C_4H_{10} increase with decreasing temperature. The values at 35, 25, 0, and −20 °C are 40 ± 3, 51 ± 4, 89 ± 8, and 77 ± 8, respectively.

The pure gas sorption data at various temperature and fugacity (*cf.* Figs. 1 and 2) can be collapsed onto a single master curve for each penetrant by plotting the ratio of the pure gas solubility data (*i.e.*, calculated using Eq. (1)) to that at infinite dilution as a function of $1/(1 + bf)$, as shown in Fig. 3(a) and (b). The pure gas infinite dilution solubility coefficient is calculated using the dual mode sorption model as follows [5]:

$$S_\infty = k_D + C'_H b \tag{7}$$

The dual mode parameters from Table 2, whose significance will be discussed shortly, are used to calculate S_∞ according to Eq. (7) and $1/(1+bf)$. The best fit line in Fig. 3(a) and (b) was estimated using the dual mode sorption model as follows:

$$\frac{S}{S_\infty} = \frac{k_D + \frac{C'_H b}{1+bf}}{k_D + C'_H b} \tag{8}$$

Rearrangement of Eq. (8) then yields:

$$\frac{S}{S_\infty} = \frac{1}{1 + C'_H b/k_D} + \frac{1}{1 + k_D/\left(C'_H b\right)} \frac{1}{1+bf} \tag{9}$$

The best fit of the data in Fig. 3(a) and (b) to Eq. (9) yields a straight line whose slope and intercept depend only on a single parameter, $C'_H b/k_D$. If this grouping is independent of temperature, then the data will lie on a straight line, as they do in this case. A least squares fit of the data in Fig. 3 to Eq. (9) determines the best effective values of $C'_H b/k_D$ to describe data. The $C'_H b/k_D$ obtained from these master curves are 6.0 ± 1.6 and 29 ± 2 for CH_4 and n-C_4H_{10}, respectively. These values agree, within experimental uncertainty, with the average $C'_H b/k_D$ values from all temperatures calculated using the dual mode parameters in Table 2, which are 6.6 ± 1.0 and 35 ± 5 for CH_4 and n-C_4H_{10}, respectively.

Table 1
CH_4 and n-C_4H_{10} dual mode parameters in PTMSP determined from pure gas sorption isotherms

T (°C)	CH_4			n-C_4H_{10}		
	k_D [a]	C'_H [b]	b [c]	k_D [a]	C'_H [b]	b [c]
−20	1.7 ± 0.2	66 ± 6	0.13 ± 0.01	211 ± 17	56 ± 2	175 ± 19
0	1.2 ± 0.1	58 ± 5	0.09 ± 0.01	97 ± 8	49 ± 2	90 ± 8
25	1.0 ± 0.1	46 ± 5	0.06 ± 0.01	37 ± 3	47 ± 2	22 ± 2
35	0.86 ± 0.05	44 ± 5	0.05 ± 0.01	27 ± 2	45 ± 2	13 ± 1

[a] $cm^3(STP)/(cm^3\,atm)$.
[b] $cm^3(STP)/cm^3$.
[c] atm^{-1}.

4.2. Mixed gas solubility

Fig. 4(a) and (b) presents pure and mixed gas sorption isotherms for CH_4 and n-C_4H_{10} in PTMSP at 35 °C as a function of CH_4 fugacity. Each mixture isotherm is determined at a nominally fixed n-C_4H_{10} fugacity. Due to the experimental methodology, the n-C_4H_{10} fugacity varies slightly over the course of each sorption isotherm, as discussed previously [12]. The n-C_4H_{10} fugacities reported in Fig. 4(a) and (b) are average values for each mixture isotherm. The uncertainties shown are standard deviations from the average values. Fig. 4(a) shows that, at similar CH_4 fugacity, CH_4 concentration sorbed in the polymer decreases as n-C_4H_{10} fugacity increases. For example, the CH_4 concentration in the polymer at 8.0 atm CH_4 fugacity is 19.8 $cm^3(STP)/cm^3$ when no n-C_4H_{10} is present. At similar CH_4 fugacity, CH_4 concentrations in the presence of 0.23 atm n-C_4H_{10} fugacity (~0.08 activity) and 1.62 atm n-C_4H_{10} fugacity (~0.54 activity) are 8.7 and 5.5 $cm^3(STP)/cm^3$, respectively. Competitive sorption effects have been observed previously during gas mixture sorption in glassy polymers [19]. Penetrant molecules compete for the limited number of sorption sites in the non-equilibrium excess volume (*i.e.*, Langmuir sites), resulting in lower gas solubilities in mixtures than in pure gases [19]. In this study, n-C_4H_{10}, which is much more soluble than CH_4 in the polymer, presumably occupies more of the sorption sites in the Langmuir region. Thus, the presence of n-C_4H_{10} reduces CH_4 sorption significantly, and consequently, decreases CH_4 mixture solubility in the polymer. On the other hand, n-C_4H_{10} solubility is not significantly affected by the presence of CH_4 in the mixture. Fig. 4(b) shows that the n-C_4H_{10} concentration is essentially unchanged as CH_4 fugacity increases. That is, methane is not condensable enough to effectively compete with n-C_4H_{10} for the limited number of Langmuir sites.

Competitive effects are observed at all temperatures studied. Fig. 5(a) and (b) presents pure and mixed gas sorption isotherms of CH_4 and n-C_4H_{10} in PTMSP at −20 °C as a function of CH_4 fugacity. The CH_4 concentration in the polymer is considerably reduced in the presence of n-C_4H_{10}, while the n-C_4H_{10} concentration remains relatively unchanged in the presence of CH_4. Mixture sorption isotherms of CH_4 and n-C_4H_{10} at 25 and 0 °C, presented in Supplementary data, exhibit similar trends.

Fig. 6(a) and (b) presents mixed gas solubility of CH_4 in PTMSP, in the limit of 0 atm of CH_4 fugacity, as a function of n-C_4H_{10} activity. The mixed gas CH_4 solubility in the limit of 0 atm CH_4 fugacity is calculated from Eqs. (1) and (5) as follows:

$$\lim_{f_A \to 0} S_A = S_{A,inf} = k_{D_A} + \frac{C'_{H_A} b_A}{1 + b_B f_B} \tag{10}$$

where the subscripts A and B refer to CH_4 and n-C_4H_{10}, respectively. The symbols are calculated from the best fit dual mode parameters for each individual mixture isotherm. The dashed lines and solid lines in Fig. 6(a) and (b) are determined using the dual mode parameters in Tables 1 and 2, respectively, which represent fits to all pure gas data and all pure and mixed gas data, respectively. The mixed gas CH_4 solubility is considerably lower than the pure gas solubility due to the competitive sorption effects discussed earlier. For example, CH_4 infinite dilution pure gas solubility in PTMSP at 25 °C is 4.0 $cm^3(STP)/(cm^3\,atm)$. In the presence of n-C_4H_{10} at an activity of 0.21, CH_4 solubility decreases by a factor of 4, to 1.0 $cm^3(STP)/(cm^3\,atm)$. At higher n-C_4H_{10} activity, CH_4 mixture solubility in the polymer apparently reaches a plateau that, consistent with the dual mode sorption model (cf. Eq. (10)), is the CH_4 k_D value at that temperature.

Fig. 7 presents pure and mixed gas solubility of n-C_4H_{10} in PTMSP as a function of n-C_4H_{10} activity and temperature. The closed symbols are from pure gas measurements, and the open symbols are data points from mixture measurements. The mixture solubilities of n-C_4H_{10} in PTMSP are close to the pure gas values. The influence of CH_4 on n-C_4H_{10} solubility is too weak to be measured in these experiments.

The mixed gas sorption isotherms can be described using the dual model sorption model for binary mixtures (*i.e.*, Eqs. (5) and (6)). The pure gas dual mode parameters recorded in Table 1 were initially used to predict mixture sorption behavior in PTMSP. The predictions from the pure gas parameters, shown as dashed lines in Fig. 6(a) and (b), overestimate the mixed gas CH_4 solubility somewhat at higher n-C_4H_{10} activity. The source of the discrepancy is the CH_4 pure gas dual mode parameters calculated from pure gas sorption measurements; these values are not completely reliable due to the lack of curvature in the CH_4 pure gas sorption isotherms. Table 2 records the best fit CH_4 and n-C_4H_{10} dual mode parameters determined by simultaneously fitting the pure and mixed gas CH_4 and n-C_4H_{10} sorption data to Eqs. (5) and (6). The model predictions using these parameters, presented in Figs. 4–7,

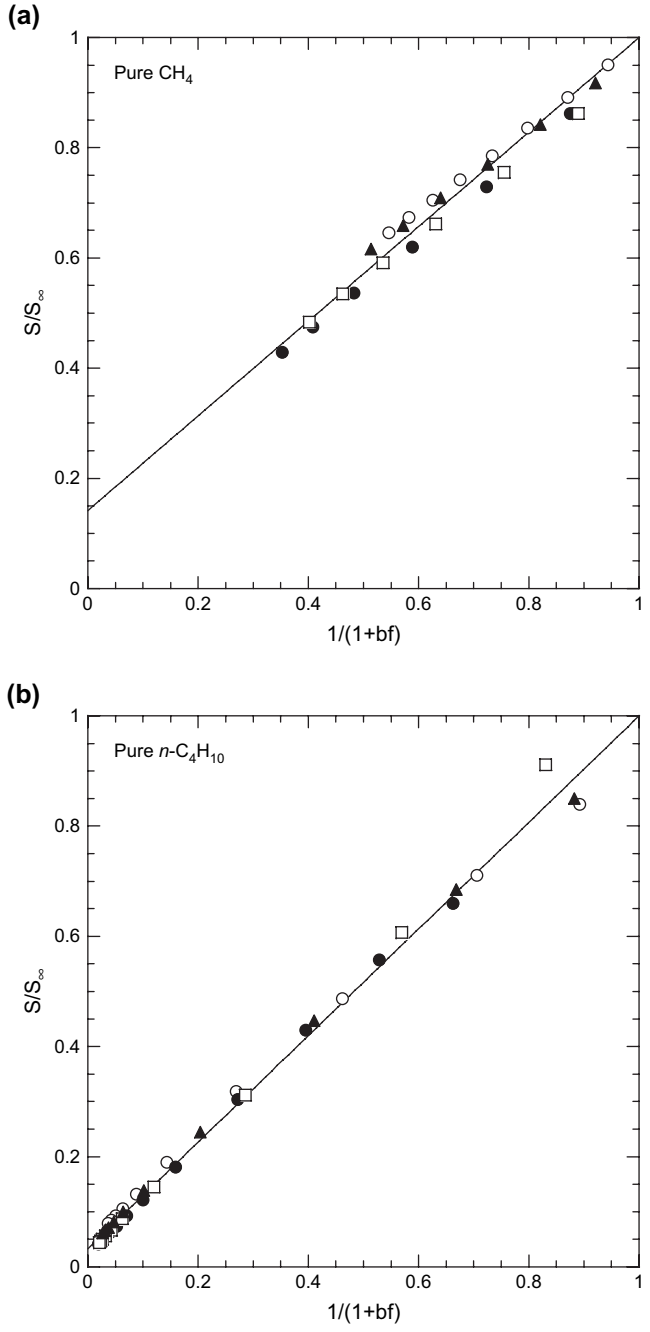

Fig. 3. The ratio of pure gas (a) CH_4 and (b) n-C_4H_{10} solubility coefficient to their infinite dilution pure gas solubility coefficients as a function of $1/(1+bf)$ at various temperatures: (○) 35 °C, (▲) 25 °C, (□) 0 °C, and (●) −20 °C. S is calculated from the pure gas sorption data in Figs. 1 and 2 using Eq. (1). S_∞ is calculated from Eq. (7) using the dual mode parameters in Table 2. The lines are fits to Eq. (9) with best fit $C'_H b/k_D$ values of 5.2 ± 1.6 and 30 ± 2 for CH_4 and n-C_4H_{10}, respectively.

describe the experimental data well. There is some disagreement between the CH_4 dual mode parameters in Table 1 and those in Table 2. The k_D values of CH_4 estimated from the pure gas data (*e.g.*, 0.86 ± 0.05 cm^3(STP)/(cm^3 atm at 35 °C) are higher than those estimated from the pure and mixed gas data (0.60 ± 0.05 cm^3(STP)/(cm^3 atm) at 35 °C). The C'_H values for CH_4 obtained from the pure gas data are, in general, slightly lower than those determined from the pure and mixed gas data. The b values estimated from the pure gas data and the mixed gas data, however, are similar. The CH_4 dual mode parameters estimated simultaneously from the pure and mixed gas data (*i.e.*, the values in Table 2) are presumably more reliable than those estimated only from pure gas sorption isotherms (*i.e.*, the values in Table 1). As shown in Fig. 6(a) and (b), CH_4 solubility reaches a plateau at higher n-C_4H_{10} activity, which indicates saturation of the Langmuir sites. In this plateau region, penetrant sorption occurs mostly in the dense equilibrium Henry's law region, and, according to the dual mode sorption model, the CH_4 solubility approaches k_D. Therefore, the mixture data provide a more accurate and reliable approximation of k_D, because, by using n-C_4H_{10} to saturate the Langmuir sites, one obtains CH_4 solubility values that are more consistent with CH_4 sorption only in the Henry's law sites. The CH_4 dual mode parameters in Table 2 agree with CH_4 pure gas parameters in the literature [5]. Our values at 35 °C are 0.60 cm^3(STP)/(cm^3 atm), 56 cm^3(STP)/cm^3, and 0.051 atm^{-1} for k_D, C'_H, and b, respectively. Merkel et al. reported values of 0.50 cm^3(STP)/cm^3 atm, 62 cm^3(STP)/cm^3, and 0.05 atm^{-1} at this temperature for k_D, C'_H, and b, respectively [5]. Srinivasan et al. [26] reported k_D, C'_H, and b values at 25 °C of 0.63 cm^3(STP)/cm^3 atm, 59 cm^3(STP)/cm^3, and 0.058 atm^{-1}, respectively, in good agreement with the parameters obtained in this study (0.68 cm^3(STP)/cm^3 atm, 56 cm^3(STP)/cm^3, and 0.061 atm^{-1}). The n-C_4H_{10} dual mode parameters estimated simultaneously from the pure and mixture data (Table 2) are essentially the same as those determined from pure gas data alone (Table 1).

The Langmuir capacity parameter, C'_H, can be used to estimate the amount of non-equilibrium excess free volume in a glassy polymer using the following expression [17]:

$$C'_H\left(\frac{M}{22,414}\right) = \frac{V_p - V_l}{V_p}\rho^* = f \times \rho^* \tag{11}$$

where C'_H has units of cm^3(STP)/cm^3, M is the molecular weight of the penetrant, V_p is the specific volume of the polymer, V_l is the specific volume of the densified polymer matrix, f is the accessible non-equilibrium excess free volume fraction, ρ^* is the condensed penetrant density, and 22,414 cm^3(STP)/mol is a conversion factor. ρ^* has been estimated as the liquid density of the pure penetrant at the experimental temperature [5]. The saturated liquid densities of n-C_4H_{10} at 35, 25, 0, and −20 °C are 0.56, 0.57, 0.60, and 0.62 g/cm^3 [27]. Based on these values and C'_H from Table 2, the excess free volume fraction in PTMSP (*i.e.*, f) from n-C_4H_{10} data is 0.18, 0.19, 0.20, and 0.22, at 35, 25, 0, and −20 °C, respectively. These values are unusually high compared to those estimated in conventional, low free volume glassy polymers, such as polycarbonate (0.04) and poly(phenylene oxide) (0.06) [17,28]. However, the excess free volume fraction estimated in this study is slightly lower than that previously reported for PTMSP: Merkel et al. reported an f value in PTMSP of 0.25 based on C_3H_8 sorption data at 35 °C [5], and Srinivasan

Table 2
CH_4 and n-C_4H_{10} dual mode parameters in PTMSP determined from both pure and mixed gas sorption isotherms

T (°C)	CH_4			n-C_4H_{10}		
	k_D [a]	C'_H [b]	b [c]	k_D [a]	C'_H [b]	b [c]
−20	1.00 ± 0.07	79 ± 7	0.12 ± 0.01	213 ± 17	53 ± 3	188 ± 20
0	0.83 ± 0.05	63 ± 5	0.10 ± 0.01	96 ± 7	47 ± 2	85 ± 9
25	0.68 ± 0.05	56 ± 5	0.06 ± 0.01	38 ± 3	43 ± 2	26 ± 3
35	0.60 ± 0.05	56 ± 5	0.05 ± 0.01	29 ± 2	40 ± 2	16 ± 2

[a] $cm^3(STP)/(cm^3\ atm)$.
[b] $cm^3(STP)/cm^3$.
[c] atm^{-1}.

et al. reported an f value of 0.24 based on CO_2 sorption data at 25 °C [26].

The temperature dependence of k_D can be described using a van't Hoff expression, as follows [29]:

$$k_D = k_{D_o}\exp\left(\frac{-\Delta H_D}{RT}\right) \tag{12}$$

where k_{D_o} is a constant, ΔH_D is the enthalpy change of sorption in the Henry's law region, R is the gas constant, and T is absolute temperature. The k_D values of CH_4 and n-C_4H_{10} recorded in Table 2 are plotted against $1/T$ in Fig. 8. Fitting these k_D values to Eq. (12) yields k_{D_o} values of $6.3 \pm 0.5 \times 10^{-2}$ and $0.27 \pm 0.02 \times 10^{-2}$ $cm^3(STP)/(cm^3\ atm)$ for CH_4 and n-C_4H_{10}, respectively. The ΔH_D of CH_4 and n-C_4H_{10} are -5.8 ± 0.5 and -24 ± 2 kJ/mol, respectively. Interestingly, these ΔH_D values are very similar to the pure gas enthalpies of sorption of CH_4 and n-C_4H_{10} (−5.8 and −23.0 kJ/mol, respectively) at infinite dilution in poly(dimethylsiloxane) (PDMS) [12]. In addition, the ΔH_D of n-C_4H_{10} in PTMSP is very close to the enthalpy of condensation, ΔH_{cond}, of n-C_4H_{10}. In this regard, the ΔH_{cond} of n-C_4H_{10} at 15 °C (*i.e.*, the median of the temperature range explored in this study) is −21.6 kJ/mol [27]. That is, ΔH_D is essentially given by the enthalpy of condensation, and its value is sensibly equal to the enthalpy of sorption in a nonpolar, rubbery polymer (*i.e.*, PDMS).

The temperature dependence of b is typically given by [29]:

$$b = b_o\exp\left(\frac{-\Delta H_b}{RT}\right) \tag{13}$$

where b_o is a constant and ΔH_b is the corresponding enthalpy change. The temperature dependence of b values for CH_4 and n-C_4H_{10} in PTMSP (Table 2) are presented in Fig. 9. The b_o values of CH_4 and n-C_4H_{10} are $6.4 \pm 0.5 \times 10^{-4}$ and $2.0 \pm 0.2 \times 10^{-4}$ atm^{-1}, respectively. The ΔH_b of CH_4 and n-C_4H_{10} are -11 ± 1 and -29 ± 2 kJ/mol, respectively. These ΔH_b values are lower (*i.e.*, more negative) than the ΔH_D values determined earlier. Similar observations have been reported in the literature [30,31]. Sorption in the Henry's law region involves separation of polymer chain segments to accommodate penetrant molecules [29]. In the Langmuir region, since the microvoids supposedly already exist, no extra energy is required to separate chains to accommodate sorption in this region [29]. As a result, sorption in the Langmuir region is less energetic than that in the Henry's law region [29], so, for the same penetrant, ΔH_b is more negative than ΔH_D. The ΔH_b of CH_4 in PTMSP is slightly higher (*i.e.*, less negative) than the CH_4 enthalpy of adsorption in porous materials (*e.g.*, zeolite, carbon membranes), which is typically between −15 and −25 kJ/mol [32–34]. Nevertheless, they are quite close to these values, which suggests a similarity between the hole-filling sorption mechanism in the Langmuir region of PTMSP and the adsorption mechanism in porous materials. For instance, the enthalpy of adsorption of CH_4 in β-zeolite with a pore size of 6–7 Å is −16 kJ/mol [35].

The isosteric enthalpy of sorption, ΔH_S^C, at a fixed penetrant concentration, C, can be calculated as follows [29]:

$$\Delta H_S^C = -R\left(\frac{d\ln S}{d(1/T)}\right)_C \tag{14}$$

Fig. 10 presents pure gas enthalpy of sorption as a function of penetrant concentration in the polymer. The ΔH_S of CH_4 is essentially independent of CH_4 concentration. The average ΔH_S^C of CH_4 over the concentration range is -14 ± 1 kJ/mol, which is lower than the enthalpy of sorption of CH_4 in liquid n-C_4H_{10} (−9.7 kJ/mol) [12] and in PDMS (−5.8 kJ/mol) [12] due to the pre-existing voids that are readily available for sorption in the Langmuir region. The ΔH_S^C of n-C_4H_{10} initially decreases with increasing n-C_4H_{10} concentration, reaches a minimum at approximately 40 $cm^3(STP)/cm^3$, and then increases with increasing n-C_4H_{10} concentration at n-C_4H_{10} concentration greater than 40 $cm^3(STP)/cm^3$. A similar trend has been reported in other glassy polymers and is consistent with the dual mode interpretation of penetrant sorption [29,36,37]. At low n-C_4H_{10} concentration, sorption occurs predominantly in the Langmuir region, in which sorption sites are readily accessible. As n-C_4H_{10} concentration increases, the Langmuir region becomes progressively more saturated, resulting in a larger fraction of the sorption occurring in the Henry's law region, in which penetrant dissolution is more energetically demanding than that in the Langmuir region since it involves the separation of polymer chain segments to accommodate penetrant molecules [37]. Consequently, the ΔH_S^C of n-C_4H_{10} increases with n-C_4H_{10} concentration (for $C > 40$ $cm^3(STP)/cm^3$) and appears to approach

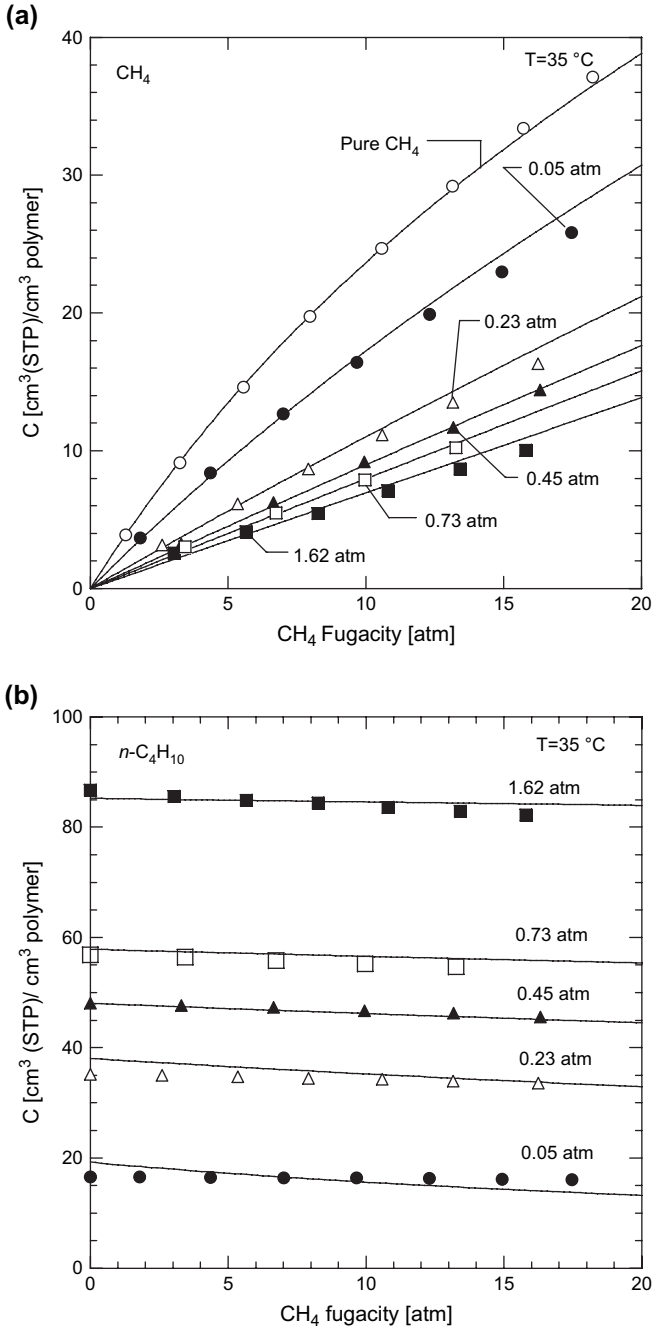

Fig. 4. Pure and mixed gas sorption isotherms of (a) CH_4 and (b) n-C_4H_{10} as a function of CH_4 fugacity at 35 °C. Each isotherm is determined at a nominally fixed n-C_4H_{10} fugacity, whose value (in atm) is given by the numbers in the figures. These n-C_4H_{10} fugacities are averages over the course of each sorption isotherm. The average n-C_4H_{10} activities (f/f_{sat}) in these isotherms are: (○) 0 (*i.e.*, pure CH_4), (●) 0.017 ± 0.003, (△) 0.08 ± 0.01, (▲) 0.15 ± 0.01, (□) 0.24 ± 0.01, and (■) 0.54 ± 0.01. f_{sat} of n-C_4H_{10} at 35 °C is 3.00 atm [24]. The uncertainties in the n-C_4H_{10} activity values represent the standard deviation of the average values over the course of the sorption experiment. The lines represent the dual mode sorption model fits using the parameters in Table 2.

the ΔH_{cond} of n-C_4H_{10} at higher n-C_4H_{10} concentration. In this study, the ΔH_S^C of n-C_4H_{10} is always lower than the ΔH_{cond} of n-C_4H_{10} throughout the concentration range explored, which means that the enthalpy of mixing of n-C_4H_{10} is exothermic. The trend in ΔH_{mix} should exhibit the same functional dependence on concentration as ΔH_S^C since ΔH_{cond} is independent of concentration. Fig. 10 also presents the ΔH_S^C of CH_4 in mixtures as a function of n-C_4H_{10} concentration in the polymer. The trend is similar to that observed for n-C_4H_{10}. As n-C_4H_{10} concentration increases, a greater fraction of CH_4 molecules partitions into the Henry's law region. As a result, CH_4 sorption in the polymer becomes energetically more difficult. The ΔH_S^C of CH_4 increases with increasing n-C_4H_{10} concentration at n-C_4H_{10} concentrations greater than 30 cm^3(STP)/cm^3. Interestingly, the minimum in ΔH_S^C for both CH_4 and n-C_4H_{10} occurs at a similar n-C_4H_{10} concentration (around 30–40 cm^3(STP)/cm^3). At n-C_4H_{10} concentrations greater than 60 cm^3(STP)/cm^3, the ΔH_S^C of CH_4 in mixtures is somewhat higher than the ΔH_S^C of CH_4 in liquid n-C_4H_{10}. The ΔH_S^C of CH_4 seems to reach an asymptotic value at higher n-C_4H_{10} concentration. At the highest n-C_4H_{10} concentration studied (110 cm^3(STP)/cm^3), the ΔH_S^C of CH_4 is -6.8 ± 0.6 kJ/mol which is close to the ΔH_S^C of CH_4 in rubbery PDMS. For reference, the ΔH_S^C of CH_4 in PDMS decreases from -5.8 kJ/mol in pure gas to -6.9 kJ/mol in the presence of 60 cm^3(STP)/cm^3 of n-C_4H_{10} in the polymer [12]. The difference in the trends between the pure and mixed gas ΔH_S^C of CH_4 in PTMSP is shown in Fig. 10. The weak concentration dependence of ΔH_S^C for pure gas CH_4 indicates that the Langmuir region is below saturation point during the measurement, which is consistent with our previous observation on this issue.

4.3. Solubility selectivity

Fig. 11(a) presents the mixed gas n-C_4H_{10}/CH_4 solubility selectivity in PTMSP as a function of n-C_4H_{10} activity in the mixture at various temperatures. The solubility selectivity decreases as n-C_4H_{10} activity and temperature increase. For example, at −20 °C, the n-C_4H_{10}/CH_4 mixed gas solubility selectivity in PTMSP decreases from 690 to 480 as n-C_4H_{10} activity increases from 0.05 to 0.24. At 35 °C, the solubility selectivity decreases from 175 to 96 as n-C_4H_{10} activity increases from 0.03 to 0.26. Basically, the n-C_4H_{10} solubility decreases more than that of CH_4 as temperature increases or as n-C_4H_{10} activity increases. Similar to the mixed gas data, the pure gas solubility selectivity also decreases with increasing n-C_4H_{10} activity and temperature. The dual mode model adequately captures these trends.

Fig. 11(b) presents the ratio of n-C_4H_{10}/CH_4 mixed gas to pure gas solubility selectivity at various temperatures. Due to the CH_4 solubility decrease in the mixture as a result of competitive sorption, the n-C_4H_{10}/CH_4 solubility selectivities determined from the mixture measurements are substantially higher than those estimated from pure gas data. These differences between pure and mixed gas solubility selectivities are even greater at higher n-C_4H_{10} activity and lower temperature. For example, at −20 °C and an n-C_4H_{10} activity of 0.73, the mixed gas solubility selectivity is approximately nine times higher than the pure gas solubility selectivity.

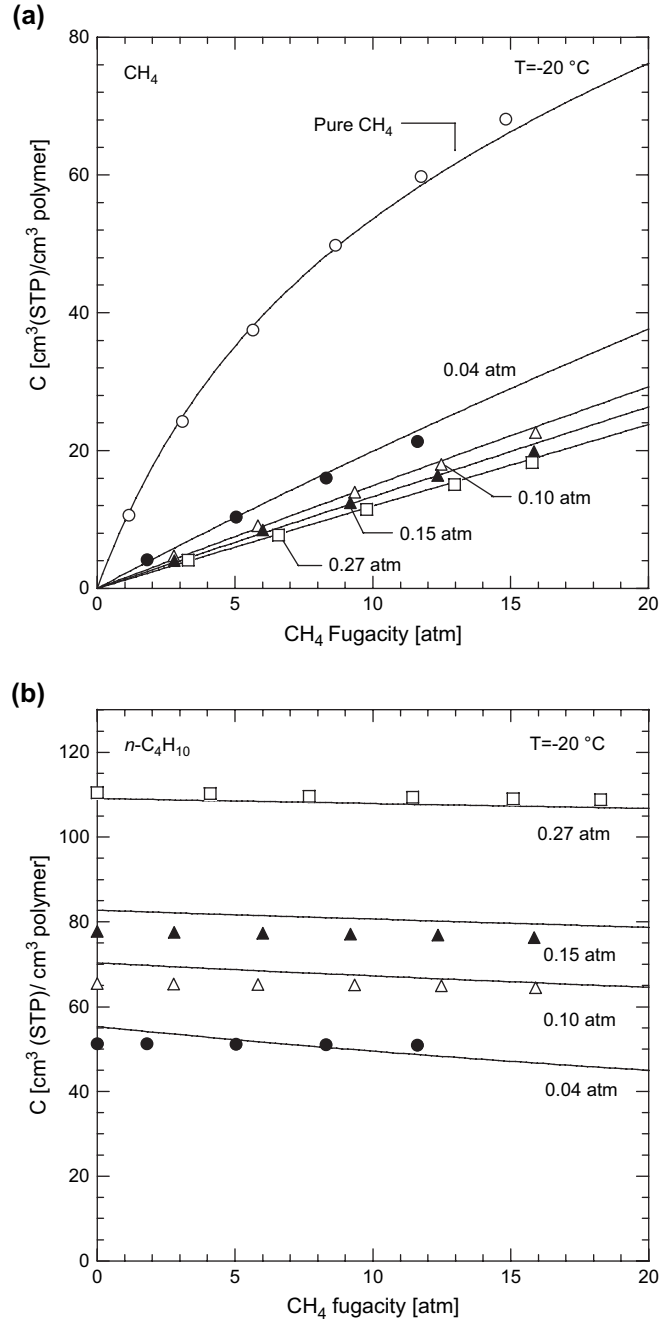

Fig. 5. Pure and mixed gas sorption isotherms of (a) CH_4 and (b) n-C_4H_{10} as a function of CH_4 fugacity at −20 °C. Each isotherm is determined at a nominally fixed n-C_4H_{10} fugacity, whose value (in atm) is given by the numbers in the figures. These n-C_4H_{10} fugacities are averages over the course of each sorption isotherm. The average n-C_4H_{10} activities (f/f_{sat}) in these isotherms are: (○) 0 (*i.e.*, pure CH_4), (●) 0.09 ± 0.01, (△) 0.22 ± 0.02, (▲) 0.34 ± 0.02, and (□) 0.61 ± 0.02. The f_{sat} of n-C_4H_{10} at −20 °C is 0.44 atm. The uncertainties represent the standard deviation of the average values. The lines represent the dual mode sorption model fits using the parameters in Table 2.

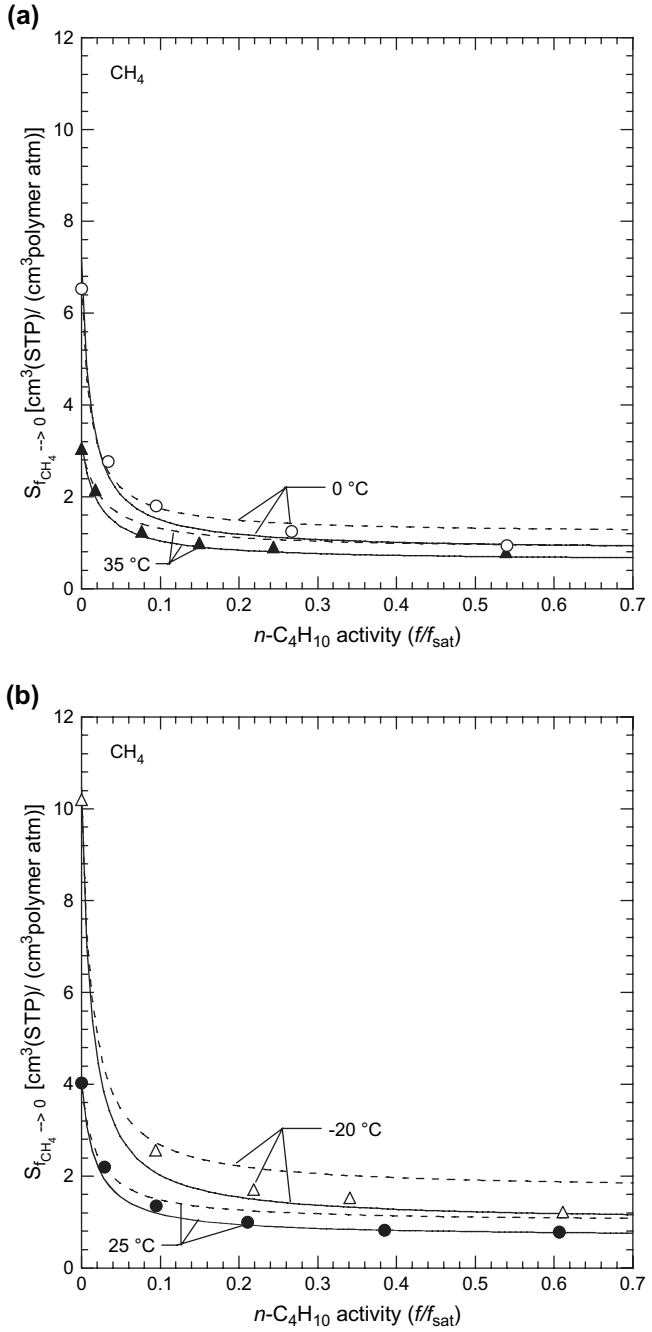

Fig. 6. CH_4 mixed gas solubility (in the limit of zero CH_4 fugacity) in PTMSP at (a) 35 and 0 °C and (b) 25 and −20 °C as a function of n-C_4H_{10} activity in mixtures. The dashed lines are the dual mode sorption model predictions using pure gas parameters from Table 1. The solid lines are the dual mode sorption model prediction using mixed gas parameters from Table 2.

4.4. Pure gas dilation

Fig. 12(a) and (b) presents pure gas CH_4 and n-C_4H_{10} induced length (*i.e.*, x-direction) dilation of PTMSP at 35 °C as a function of fugacity. ΔL_x is the change in polymer length during the measurements: $\Delta L_x = L_x - L_{x,o}$. $L_{x,o}$ is the initial penetrant-free pure polymer sample length at the experimental temperature, and L_x is the polymer sample length when exposed to gas. Similarities between the sorption and desorption cycles in the dilation isotherms indicate only very slight hysteresis during the measurements. The error bars were determined using the propagation of errors method [25].

Fig. 13 presents the length and width (*i.e.*, y-direction) dilation of two sheets of PTMSP in liquid methanol (at unit

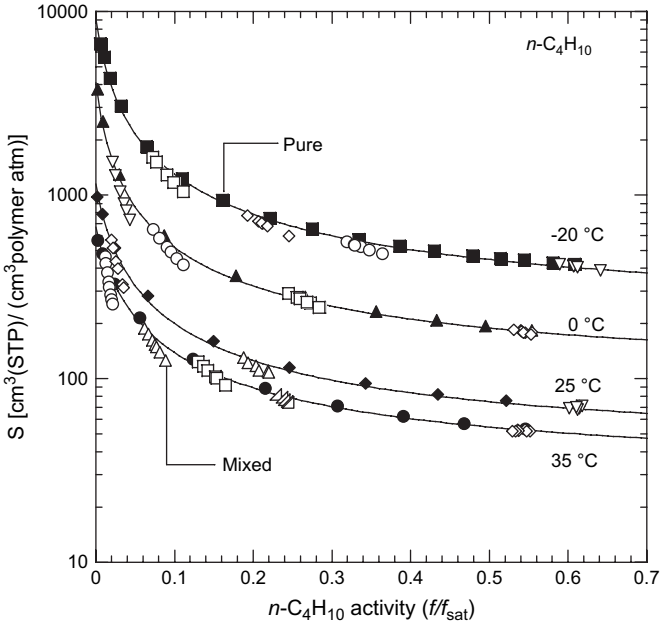

Fig. 7. Pure and mixed gas n-C_4H_{10} solubility in PTMSP as a function of n-C_4H_{10} activity and temperature. The closed symbols represent pure gas data. The open symbols represent mixed gas data at various CH_4 fugacities. The solid lines represent prediction of the dual mode sorption model using parameters from Table 2.

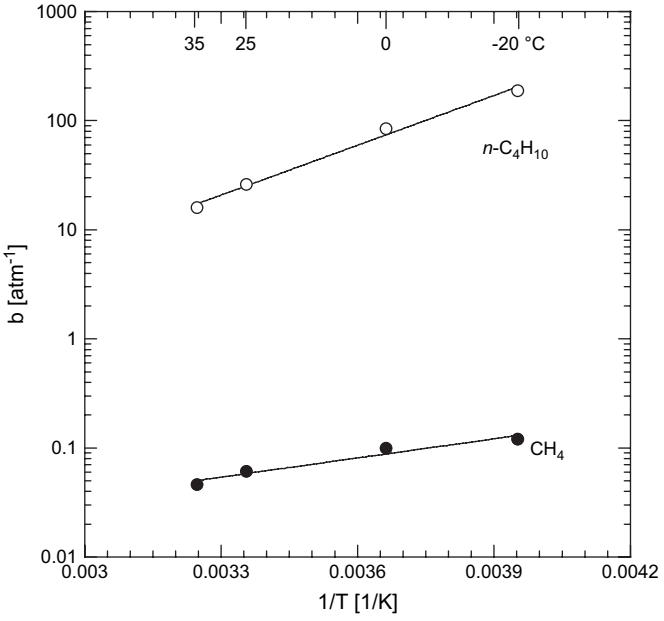

Fig. 9. The effect of temperature on b of CH_4 and n-C_4H_{10} in PTMSP. The dashed lines are fits from Eq. (13) with $b_{\infty} = 6.4 \pm 0.5 \times 10^{-4}$ atm^{-1} and $\Delta H_b = -11 \pm 1$ kJ/mol for CH_4, and $k_{D_{\infty}} = 2.0 \pm 0.2 \times 10^{-4}$ atm^{-1} and $\Delta H_b = -29 \pm 2$ kJ/mol for n-C_4H_{10}.

activity) at 25 °C. The initial (*i.e.*, dry) films are approximately square. Fig. 13 shows that the polymer dilation in the x- and y-direction is essentially the same during methanol swelling. Based on this observation, it is reasonable to assume that, during n-C_4H_{10} sorption, where the activity is always lower than unit activity, the polymer dilations are similar in the x- and y-direction.

The thickness (*i.e.*, z-direction) and length (*i.e.*, x-direction) dilation of the polymer during n-C_4H_{10} sorption at 25 and 0 °C are shown in Fig. 14(a) and (b). At similar n-C_4H_{10} fugacity, the thickness dilation is perhaps slightly higher than that of

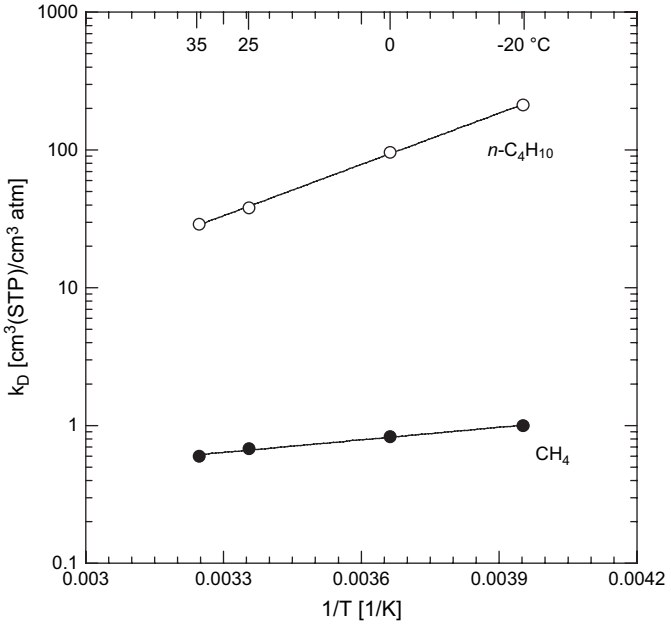

Fig. 8. The effect of temperature on k_D of CH_4 and n-C_4H_{10} in PTMSP. The dashed lines are fits from Eq. (12) with $k_{D_{\infty}} = 6.3 \pm 0.5 \times 10^{-2}$ cm^3(STP)/(cm^3 atm) and $\Delta H_D = -5.8 \pm 0.5$ kJ/mol for CH_4, and $k_{D_{\infty}} = 0.27 \pm 0.02 \times 10^{-2}$ cm^3(STP)/(cm^3 atm) and $\Delta H_D = -24 \pm 2$ kJ/mol for n-C_4H_{10}.

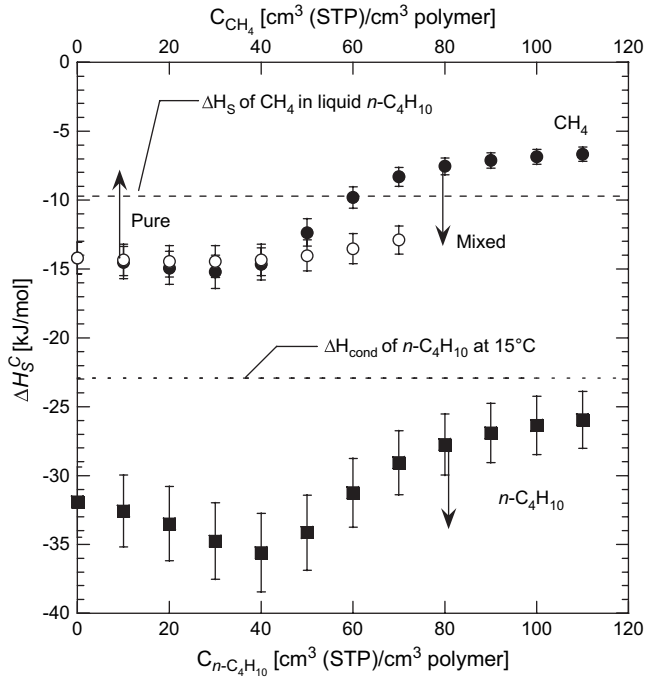

Fig. 10. The effect of concentration on CH_4 (pure and mixed gas) and n-C_4H_{10} isosteric enthalpy of sorption in PTMSP. The error bars are estimated using the propagation of errors method [25].

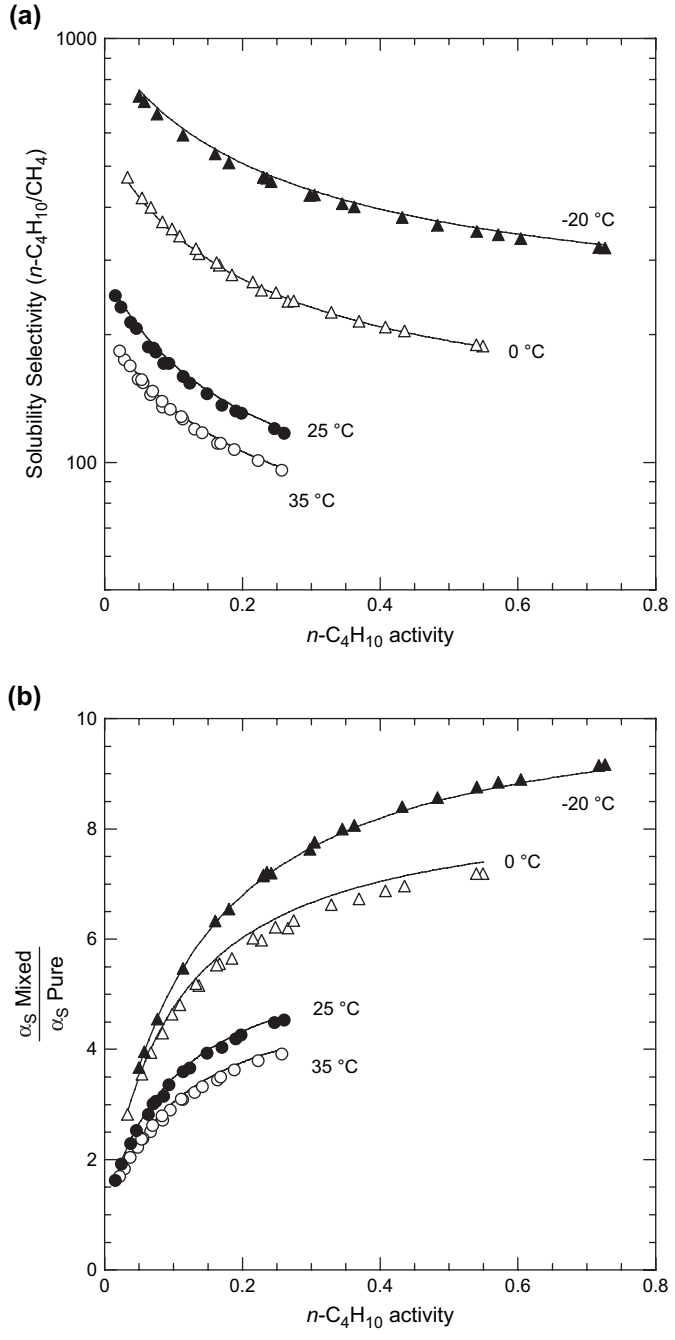

Fig. 11. (a) Mixed gas n-C_4H_{10}/CH_4 solubility selectivity in PTMSP as a function of n-C_4H_{10} activity in the mixture. (b) Ratio of n-C_4H_{10}/CH_4 mixed gas to pure gas solubility selectivity in PTMSP. The pure gas solubility selectivity is calculated from n-C_4H_{10} pure gas solubility at different n-C_4H_{10} activity values and CH_4 pure gas solubility in the limit of zero CH_4 fugacity. The lines represent predictions of the dual mode sorption model using parameters from Table 2.

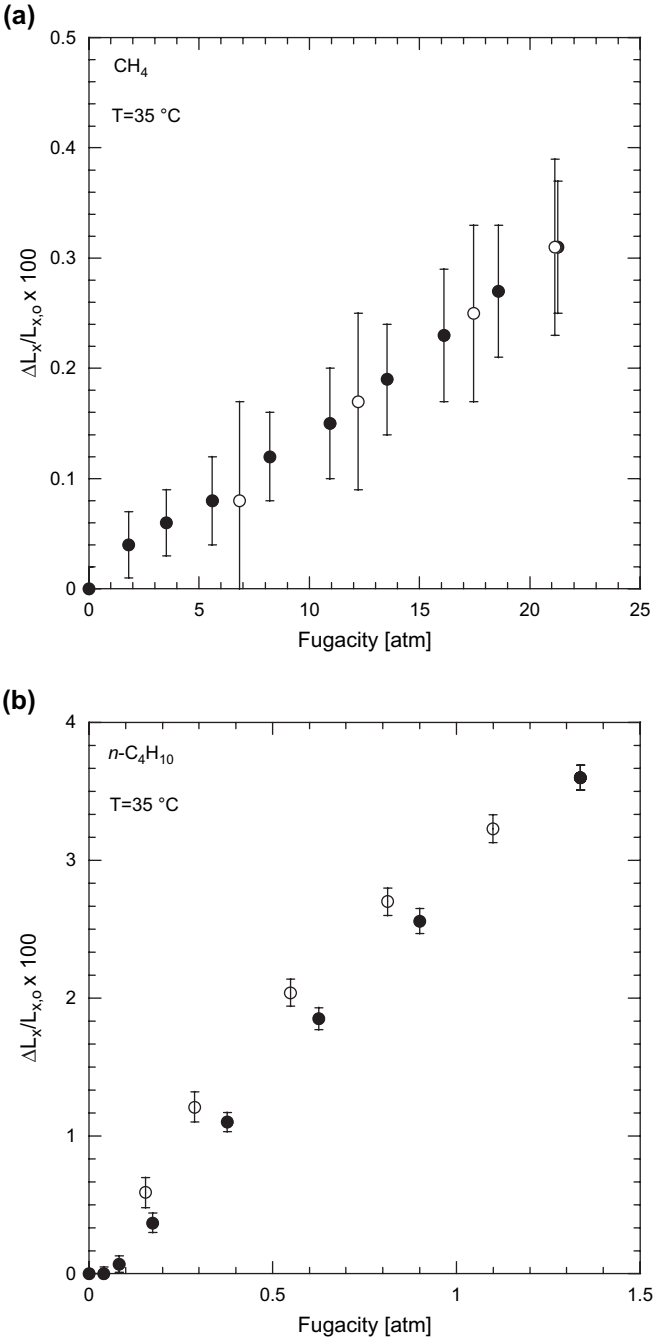

Fig. 12. Pure gas (a) CH_4 and (b) n-C_4H_{10} induced length (*i.e.*, x-direction) dilation of PTMSP at 35 °C as a function of fugacity. The open symbols represent the data obtained as gas pressure was increased. The filled symbols are the data obtained as gas pressure was decreased.

the length. However, due to limitation of our apparatus, the uncertainty in the thickness measurements is considerably higher than that in the length dilation measurements. In any event, the dilation is, at least, approximately isotropic.

By assuming that dilation is isotropic in the x and y (*i.e.*, length and width) directions, the change in polymer volume relative to the initial pure polymer volume, $\Delta V/V_o$, can be calculated as follows [12]:

$$\frac{\Delta V}{V_o} = \left(\frac{L_x}{L_{x,o}}\right)^2 \left(\frac{L_z}{L_{z,o}}\right) - 1 \tag{15}$$

where $L_{z,o}$ is the initial penetrant-free pure polymer sample length at the temperature of the experiment, and L_z is the polymer sample length when exposed to gas. $\Delta V/V_o$ can also be estimated using only the length dilation data and assuming isotropic expansion as follows [12]:

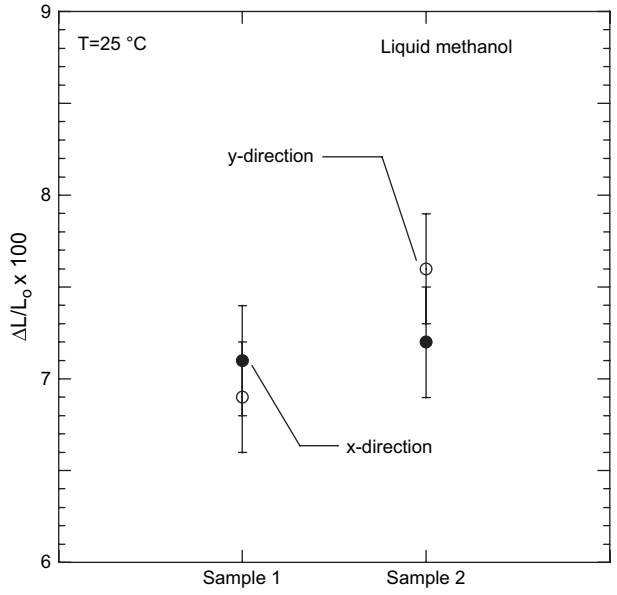

Fig. 13. Length (*i.e.*, *x*-direction) and width (*i.e.*, *y*-direction) dilation of PTMSP films in liquid methanol. The closed symbols are the length dilation data. The open symbols are the width dilation data. The dimensions of sample 1 were 6.59 cm × 6.61 cm × 300 μm and those of sample 2 were 4.74 cm × 4.72 cm × 300 μm.

$$\frac{\Delta V}{V_o} = \left(\frac{L_x}{L_{x,o}}\right)^3 - 1 \tag{16}$$

The change in polymer volume during dilation, estimated using the length and thickness dilation data (Eq. (15)), is compared to that estimated only using the length dilation (Eq. (16)) in Fig. 15(a) and (b). They agree well within the experimental uncertainty. Consequently, the change in the polymer volume can be reasonably estimated using only the length dilation data, which have significantly lower uncertainty than the thickness dilation data, and by assuming isotropic expansion. The remaining polymer volume dilation data have been calculated in this way. Pure gas dilation isotherms for CH_4 and n-C_4H_{10} are presented in Fig. 16(a) and (b).

The experimental sorption and dilation data can be combined to determine the penetrant partial molar volume in the polymer. The partial molar volume is defined as [38]:

$$\overline{V}_i \equiv \left(\frac{\partial V}{\partial n_i}\right)_{T,p,n_{j\neq i}} \tag{17}$$

where n_i is the number of moles of component i in the mixture, and V is the total mixture volume. For a gas–polymer mixture, the partial molar volume of the penetrant is estimated from dilation data as follows [16]:

$$\overline{V}_i = 22,414\left[\frac{\mathrm{d}}{\mathrm{d}p}\left(\frac{\Delta V}{V_o}\right) + \beta\right]\frac{\mathrm{d}p}{\mathrm{d}C} \tag{18}$$

where p is pressure and β is the isothermal compressibility of the polymer, which is usually small enough, especially for glassy polymers, to be neglected [7].

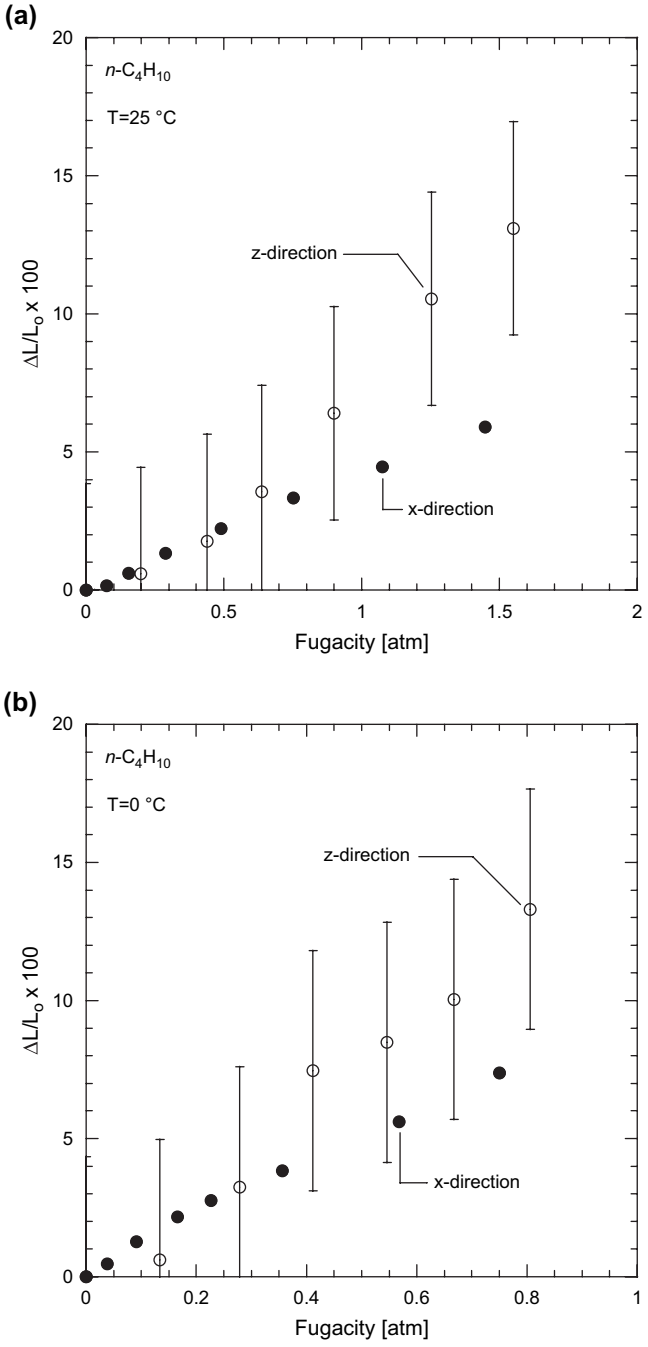

Fig. 14. Pure gas n-C_4H_{10} induced length (*i.e.*, *x*-direction) and thickness (*i.e.*, *z*-direction) dilation of PTMSP at (a) 25 °C and (b) 0 °C. The open symbols represent the thickness dilation data. The filled symbols are the length dilation data.

Fig. 17(a) and (b) presents the pure gas partial molar volumes of CH_4 and n-C_4H_{10} in PTMSP as functions of concentration at temperatures from −20 to 35 °C. The concentrations of CH_4 and n-C_4H_{10} in PTMSP are determined from the pure gas sorption data. In general, CH_4 pure gas partial molar volume slightly increases with increasing CH_4 concentration. n-C_4H_{10} pure gas partial molar volume increases, to a greater extent than CH_4, with increasing n-C_4H_{10} concentration. The

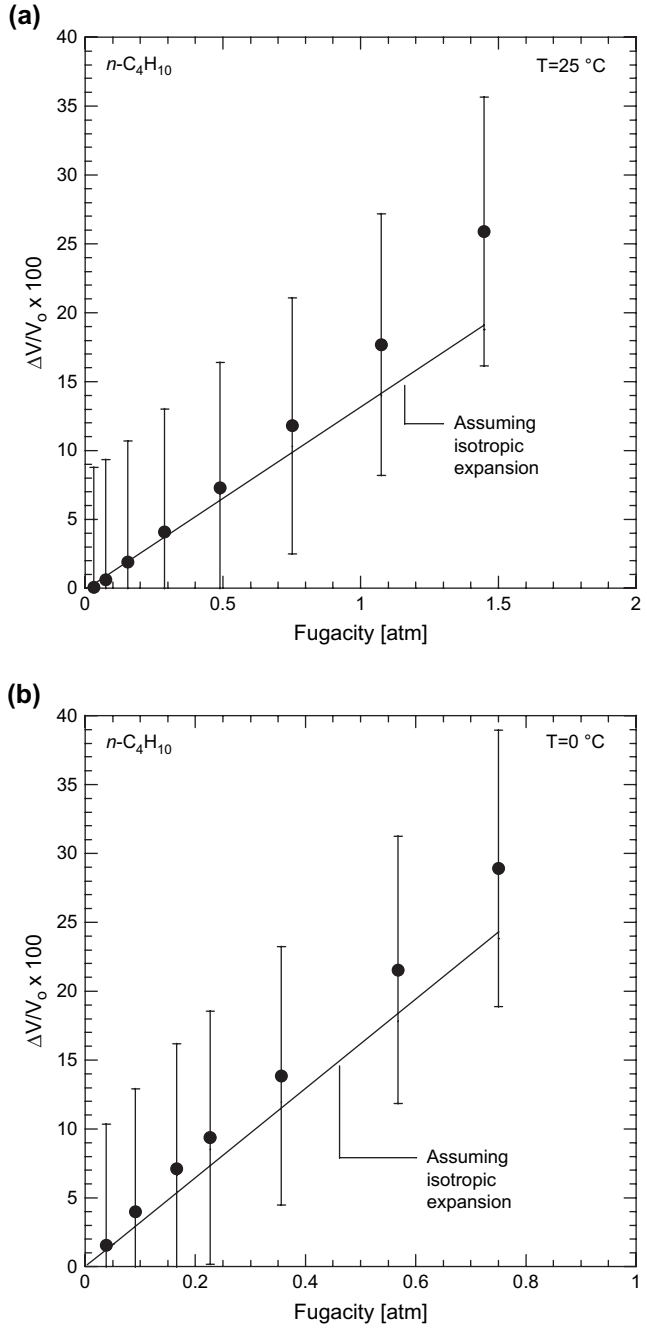

Fig. 15. The change in polymer volume during pure gas n-C_4H_{10} sorption in PTMSP at (a) 25 °C and (b) 0 °C. The data points are volume dilation estimated from the length and thickness dilation data using Eq. (15). The lines are calculated from Eq. (16) using the length dilation data and assuming isotropic expansion.

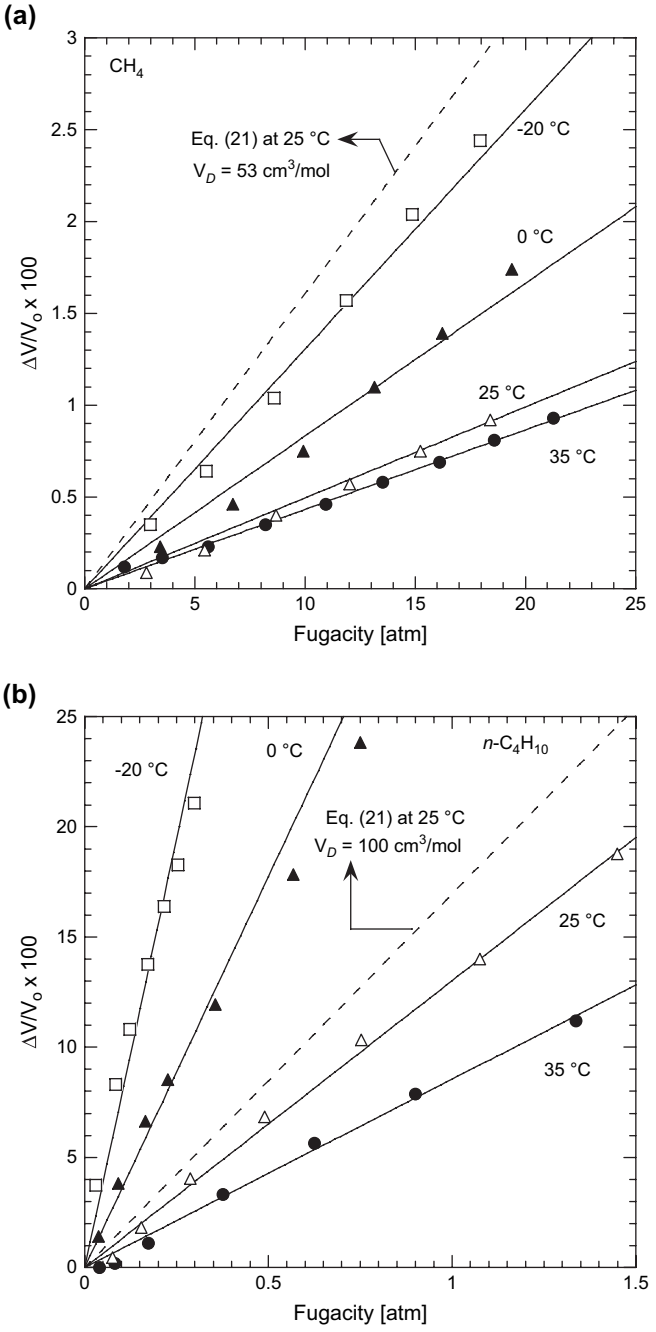

Fig. 16. Pure gas (a) CH_4 and (b) n-C_4H_{10} induced-dilation of PTMSP as a function of fugacity from −20 to 35 °C. The solid lines are predictions from Eq. (21) with the best fit V_D recorded in Table 3. The dashed line represents the estimated volume dilation at 25 °C using Eq. (21) with (a) $V_D = 53$ cm^3/mol for CH_4, and $V_D = 100$ cm^3/mol for n-C_4H_{10}.

partial molar volumes of CH_4 and n-C_4H_{10} in PTMSP are much lower than those in liquids. For comparison, the average partial molar volume of CH_4 in five organic solvents at 25 °C is 53 cm^3/mol [39]. The pure liquid molar volume of n-C_4H_{10} at 20 °C is 100 cm^3/mol [24]. The extraordinarily low penetrant partial molar volumes in glassy PTMSP has been explained by a hole-filling sorption mechanism implicitly expressed in the dual mode sorption model [21]. Fleming and Koros suggested that, ideally, only the fraction of the total sorption associated with the actual separation of chain segments to accommodate the penetrant would cause volume dilation [21]. If the sorption in the Langmuir sites corresponds to a true hole-filling process, the polymer volume dilation should arise only from sorption in the Henry's law region (*i.e.*, C_D). This idea can qualitatively explain the low partial molar volume values in glassy PTMSP compared to low molecular weight systems, in which no such hole-filling mechanism occurs.

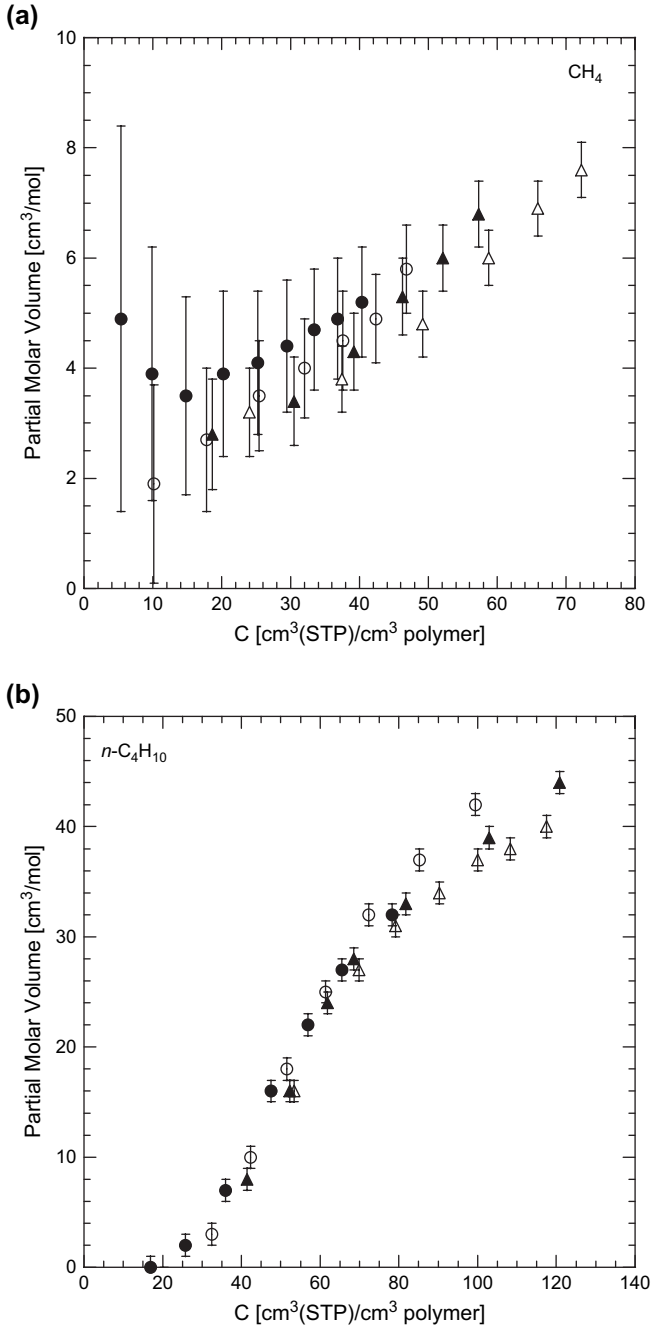

Fig. 17. Pure gas partial molar volumes of (a) CH_4 as a function of CH_4 concentration and (b) n-C_4H_{10} as a function of n-C_4H_{10} concentration in the polymer. The various symbols represent values at different temperatures: (●) 35 °C, (○) 25 °C, (▲) 0 °C, and (△) −20 °C.

The small lag in PTMSP dilation at a very low n-C_4H_{10} fugacity (Fig. 12(b)) and the near-zero partial molar volume of n-C_4H_{10} at low n-C_4H_{10} concentration (Fig. 17(b)) can be rationalized using the same hole-filling concept. Based on the dual mode sorption model, the relative penetrant populations in the Henry's law and Langmuir regions can be estimated, using the dual mode parameter in Table 2, as follows:

$$\frac{C_H}{C_D} = \frac{C'_H b}{k_D(1+bf)} \tag{19}$$

Table 3
Best fit V_D of CH_4 and n-C_4H_{10} in PTMSP at various temperatures

T (°C)	V_D (cm³/mol)	
	CH_4	n-C_4H_{10}
−20	29 ± 3	82 ± 6
0	22 ± 3	83 ± 5
25	16 ± 3	77 ± 6
35	16 ± 3	66 ± 5

In the limit of zero fugacity, Eq. (19) can be written as follows:

$$\lim_{f\to 0} \frac{C_H}{C_D} = \frac{C'_H b}{k_D} \tag{20}$$

Penetrant sorption in glassy polymers, especially for condensable vapors, always favors sorption in the Langmuir region over the Henry's law region at the limit of low fugacity. For example, at 35 ° and in the limit of zero fugacity, the n-C_4H_{10} concentration sorbed in the Langmuir region is approximately 22 times that sorbed in the Henry's law region. Since most n-C_4H_{10} sorption at low n-C_4H_{10} fugacity in PTMSP takes place in the Langmuir region, there should be no significant dilation observed at this n-C_4H_{10} fugacity range, as shown in Fig. 12(b). And, as a result, the estimated n-C_4H_{10} partial molar volume is practically zero at low n-C_4H_{10} concentrations, as shown in Fig. 17(b). As fugacity increases, the ratio C_H/C_D calculated using Eq. (19) decreases. In other words, the fraction of penetrant sorption in the Henry's law region increases with fugacity. This trend is consistent with the dilation data in Fig. 17(a) and (b), where the partial molar volumes of CH_4 and n-C_4H_{10} increase with increasing concentration (or fugacity).

Fleming and Koros suggested that the pure gas dilation data can be predicted from the concentration of penetrant sorbed in the Henry's law region [21]:

$$\frac{\Delta V}{V_o} = \frac{C_D}{22,414} V_D = \frac{k_D f}{22,414} V_D \tag{21}$$

where V_D is the penetrant partial molar volume in the Henry's law region. Ideally, V_D should be similar to the penetrant partial molar volume in low molecular weight systems [21]. The

Table 4
Best fit V_D of various penetrants at 35 °C

	V_D (cm³/mol)			
	CO_2	CH_4	n-C_4H_{10}	n-C_9H_{20}
PTMSP	6.2[a]	16	66	148[b]
AF2400[c]	14	–	–	–
Polycarbonate[d]	46	48	–	–
Liquid	46[e]	53[e]	100[f]	179[f]

[a] Pope et al. [7].
[b] Witchey-Lakshmanan et al. [40].
[c] De Angelis et al. [41].
[d] Fleming [42].
[e] Partial molar volumes in organic liquids at 25 °C [39].
[f] Pure liquid molar volume at 20 °C [24].

dashed lines in Fig. 16(a) and (b) represent pure gas volume dilation of CH_4 and n-C_4H_{10} at 25 °C calculated from Eq. (21), using the k_D values of CH_4 and n-C_4H_{10} at 25 °C from Table 2, the average partial molar volume of CH_4 in five organic solvents at 25 °C (53 cm^3/mol) [39] as V_D of CH_4, and the pure liquid molar volume of n-C_4H_{10} at 20 °C (100 cm^3/mol) [24] as V_D of n-C_4H_{10}. These values of V_D substantially overestimate the polymer volume dilation at 25 °C. The solid lines in Fig. 16(a) and (b) are predictions from Eq. (21) using best fit V_D values at each temperature recorded in Table 3. The best fit V_D values are still considerably lower than the partial molar volumes of CH_4 and n-C_4H_{10} in low molecular weight systems.

The same results are also observed when Eq. (21) is used to fit other PTMSP dilation data in the literature [7,40]. The best fit V_D values of CO_2 in PTMSP at 35 °C (6.2 cm^3/mol) is well below the CO_2 partial molar volume in liquids (46 cm^3/mol) [7]. The best fit V_D values of n-C_9H_{20} in PTMSP at 35 °C is 17% lower than the liquid molar volume of n-C_9H_{20} at the same temperature [40]. These values are presented in Table 4 which also compares the V_D values in poly(2,2-bistrifluoromethyl-4,5-difluoro-1,3-dioxole-*co*-tetrafluoroethylene) (AF2400),

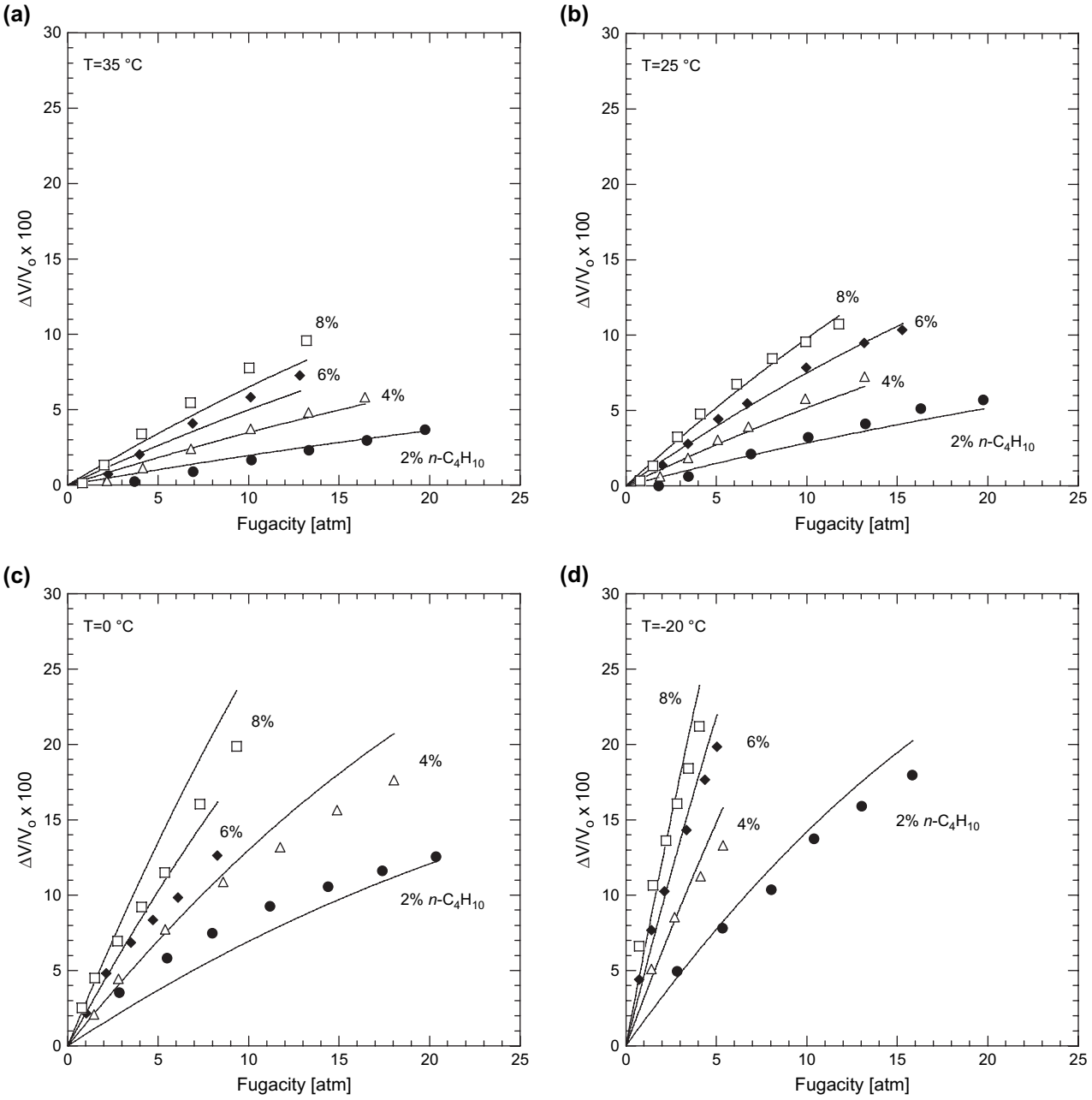

Fig. 18. n-C_4H_{10}/CH_4 mixture dilation in PTMSP at (a) 35 °C, (b) 25 °C, (c) 0 °C, and (d) −20 °C, as a function of total mixture fugacity. The solid lines are predictions from Eq. (22) using k_D values from Table 2 and V_D values from Table 3. The numbers beside the data points represent the mole percent of n-C_4H_{10} in the gas mixture.

a glassy polymer with very high fractional free volume (~0.32) [37] similar to PTMSP, and in polycarbonate, a conventional, low free volume glassy polymer. Similar to PTMSP, the best fit V_D of CO_2 in AF2400 (16 cm^3/mol) is considerably lower than the CO_2 partial molar volume in liquid [41]. In contrast, the best fit V_D values for CO_2 and CH_4 in low free volume polycarbonate are practically the same as their molar volumes in liquids [21,42]. The dense Henry's law region in high free volume glassy polymers, such as PTMSP and AF2400 could contain free volume elements that are large enough for some penetrant molecules to fill without introducing as much swelling as in a dense material such as a liquid, a low free volume glassy polymer, or a rubbery polymer. As penetrant size increases, this effect presumably diminishes, and V_D becomes more similar to the partial molar volume in liquids. For example, the V_D of CO_2, CH_4, n-C_4H_{10} and n-C_9H_{20} (*i.e.*, increasing penetrant critical volume) in PTMSP are 13, 30, 66 and 83%, respectively, of their partial molar volumes in liquids. Although using Eq. (21) with the penetrant partial molar volume in liquids as V_D provides reasonable dilation prediction in conventional, low free volume glassy polymers, there are also cases where this method underestimates the dilation in such polymers [31]. This effect has been ascribed to swelling of the polymer by penetrants in the Langmuir as well as Henry's law sites. In this case, the best fit V_D values are greater than the partial molar volumes in liquids. In summary, more theoretical and experimental studies are needed to better understand the swelling of glassy polymers.

4.5. Mixed gas dilation

PTMSP dilation isotherms as a function of fugacity for different n-C_4H_{10}/CH_4 mixtures at various temperatures are presented in Fig. 18(a)–(d). These mixture isotherms can be estimated reasonably well from the pure gas sorption and dilation data, using the following extension of Eq. (21):

$$\frac{\Delta V}{V_o} = \frac{k_{D_A} f_A}{22,414} V_{D_A} + \frac{k_{D_B} f_B}{22,414} V_{D_B} \tag{22}$$

where the subscripts A and B represent CH_4 and n-C_4H_{10}, respectively. V_{D_A} and V_{D_B} are the partial molar volumes of CH_4 and n-C_4H_{10}, respectively, in the Henry's law region, determined from pure gas measurements (*cf.*, Table 3). The solid lines in Fig. 18(a)–(d), which represent predictions of Eq. (22), describe the experimental mixture dilation data reasonably well.

5. Conclusions

Competitive sorption effects in PTMSP considerably reduce CH_4 solubility in mixtures with n-C_4H_{10}. n-C_4H_{10}, which is more condensable than CH_4 and preferentially sorbed in the polymer, occupies many of the Langmuir sorption sites, thereby reducing the CH_4 sorption capacity, and, consequently, decreases CH_4 mixture solubility. On the other hand, n-C_4H_{10} solubility is not significantly affected by the presence of CH_4 in the mixture. The dual mode mixture sorption model captures this competitive effect and is able to satisfactorily describe the experimental mixture sorption data. The n-C_4H_{10}/CH_4 mixture solubility selectivity decreases as n-C_4H_{10} decreases and temperature increases. The solubility selectivities determined from mixed gas measurements are significantly higher than those estimated from pure gas measurements due to the presence of n-C_4H_{10} reducing the concentration of CH_4 dissolved in the polymer.

As suggested previously, the pure and mixed gas volume dilation in glassy PTMSP is attributed only to the swelling in the Henry's law region. The penetrant partial molar volumes of CH_4 and n-C_4H_{10} in the Henry's law region do not change significantly in pure or mixed gas environments. The mixed gas dilation in PTMSP can be described reasonably using an additive model that ascribes polymer dilation only to those penetrant molecules sorbed in the Henry's Law regions of the polymer. However, the effective partial molar volumes of CH_4 and n-C_4H_{10} required to describe the data are markedly lower than the values expected based on the partial molar volumes of these penetrants in liquids or rubbery polymers, suggesting that these molecules sorb into even the Henry's law regions of the polymer with relatively little polymer swelling.

Acknowledgements

We gratefully acknowledge partial support of this work by the U.S. Department of Energy (grant no. DE-FG03-02ER15362) and the National Science Foundation (grant no. CTS-0515425).

Appendix. Supplementary data

Supplementary data associated with this article can be found, in the online version, at doi:10.1016/j.polymer.2007.07.057.

References

[1] Baker RW. Membrane technology and applications. 2nd ed. New York: John Wiley & Sons; 2004.
[2] Rojey A, Jaffret C, Cornot-Gandolphe S, Durand B, Jullian S, Valais M. Natural gas production processing transport. Paris: Editions Technip; 1997.
[3] Merkel TC, Bondar VI, Nagai K, Freeman BD, Pinnau I. Journal of Polymer Science Part B: Polymer Physics 2000;38:415–34.
[4] Kamiya Y, Naito Y, Terada K, Mizoguchi K, Tsuboi A. Macromolecules 2000;33:3111–9.
[5] Merkel TC, Bondar V, Nagai K, Freeman BD. Journal of Polymer Science Part B: Polymer Physics 2000;38:273–96.
[6] Morisato A, Freeman BD, Pinnau I, Casillas CG. Journal of Polymer Science Part B: Polymer Physics 1996;34:1925–34.
[7] Pope DS, Koros WJ, Hopfenberg HB. Macromolecules 1994;27:5839–44.
[8] Ghisellini M, Quinzi M, Giacinti Baschetti M, Doghieri F, Costa G, Sarti GC. Desalination 2002;149:441–5.
[9] Witchey-Lakshmanan LC, Hopfenberg HB, Chern RT. Journal of Membrane Science 1990;48:321–31.
[10] Pinnau I, He Z. Journal of Membrane Science 2004;244:227–33.

[11] Pinnau I, Casillas CG, Morisato A, Freeman BD. Journal of Polymer Science Part B: Polymer Physics 1996;34:2613–21.
[12] Raharjo RD, Freeman BD, Sanders ES. Journal of Membrane Science 2007;292:45–61.
[13] Pinnau I, Toy LG. Journal of Membrane Science 1996;116:199–209.
[14] Matteucci S, Yampolskii Y, Freeman BD, Pinnau I. Transport of gases and vapors in glassy and rubbery polymers. In: Yampolskii Y, Pinnau I, Freeman BD, editors. Materials science of membranes for gas and vapor separation. Chichester: John Wiley & Sons, Ltd; 2006. p. 1–47.
[15] van Krevelen DW. Properties of polymers: their correlation with chemical structures; their numerical estimation and prediction from additive group contribution. 3rd ed. Amsterdam: Elsevier Science; 1990.
[16] Prausnitz JM, Lichtenthaler RN, de Azevedo EG. Molecular thermodynamics of fluid-phase equilibria. 3rd ed. Upper Saddle River, NJ: Prentice-Hall, Inc.; 1999.
[17] Koros WJ, Chan AH, Paul DR. Journal of Membrane Science 1977; 2:165–90.
[18] Sanders ES. Ph.D. Dissertation, North Carolina State University; 1983.
[19] Sanders ES, Koros WJ, Hopfenberg HB, Stannett V. Journal of Membrane Science 1984;18:53–74.
[20] Nagai K, Nakagawa T. Journal of Membrane Science 1995;105:261–72.
[21] Fleming GK, Koros WJ. Macromolecules 1986;19:2285–91.
[22] McDowell CC, Freeman BD, McNeely GW. Polymer 1999;40:3487–99.
[23] Pope DS, Koros WJ, Fleming GK. Journal of Polymer Science Part B: Polymer Physics 1989;27:1173–7.
[24] Poling BE, Prausnitz JM, O'Connell JP. The properties of gases and liquids. 5th ed. New York, NY: McGraw-Hill; 2001.
[25] Bevington PR. Data reduction and error analysis for the physical sciences. 3rd ed. New York, NY: McGraw-Hill; 2002.
[26] Srinivasan R, Auvil SR, Burban PM. Journal of Membrane Science 1994;86:67–86.
[27] DIPPR Physical and thermodynamic properties, http://dippr.byu.edu/public/chemsearch.asp.
[28] Toi K, Morel G, Paul DR. Journal of Applied Polymer Science 1982;27:2997–3005.
[29] Koros WJ, Paul DR, Huvard GS. Polymer 1979;20:956–60.
[30] Michaels AS, Vieth WR, Barrie JA. Journal of Applied Physics 1963;34:13–20.
[31] Wang J-S, Kamiya Y. Journal of Membrane Science 1995;98:69–76.
[32] Buss E. Gas Separation and Purification 1995;9:189–97.
[33] Vigne-Maeder F, Auroux A. Journal of Physical Chemistry 1990;94: 316–22.
[34] Al-Baghli NA, Loughlin KF. Journal of Chemical Engineering Data 2005;50:843–8.
[35] Li P, Tezel H. Microporous and Mesoporous Materials 2007;98:94–101.
[36] Barrie JA, Munday K, Williams M. Organic Coatings and Plastics Chemistry 1978;39:187–91.
[37] Merkel TC, Bondar V, Nagai K, Freeman BD, Yampolskii Y. Macromolecules 1999;32:8427–40.
[38] Smith JM, Ness HCV, Abbott MM. Introduction to chemical engineering thermodynamics. 6th ed. New York, NY: McGraw-Hill; 2001.
[39] Horiuti J. Scientific Papers of the Institute of Physical and Chemical Research 1931;17:125–256.
[40] Witchey-Lakshmanan LC, Hopfenberg HB, Chern RT. Journal of Polymer Science Part B: Polymer Physics 1993;31:1545–53.
[41] De Angelis MG, Merkel TC, Bondar VI, Freeman BD, Doghieri F, Sarti GC. Macromolecules 2002;35:1276–88.
[42] Fleming GK. Ph.D. Dissertation, University of Texas at Austin; 1988.